



ELSEVIER

Contents lists available at ScienceDirect

Atmospheric Research

journal homepage: www.elsevier.com/locate/atmosres

Historical evaluations and simulations of precipitation over East Africa from Rossby centre regional climate model

Brian Ayugi^{a,b}, Guirong Tan^{a,*}, Gnim Tchelim Gnitou^{a,c}, Moses Ojara^{a,d}, Victor Ongoma^{a,e}

^a Key Laboratory of Meteorological Disaster, Collaborative Innovation Center on Forecast and Evaluation of Meteorological Disasters, Ministry of Education, Nanjing, University of Information Science and Technology, Nanjing 210044, China

^b College of Atmospheric Sciences, Nanjing University of Information Science and Technology, Nanjing, Jiangsu 210044, China

^c School of Computer and Software, Nanjing University of Information Science and Technology, Jiangsu, Nanjing 210044, China

^d Uganda National Meteorological Authority, Clement Hill Road, P.O. Box 7025, Kampala, Uganda

^e School of Geography, Earth Science and Environment, The University of the South Pacific, Laucala Campus Private Bag, Suva, Fiji

ARTICLE INFO

Keywords:

CORDEX

Greater Horn of Africa

Precipitation

Regional climate models

Rossby centre atmospheric models

ABSTRACT

This study assesses the performance of ten Regional Climate Model (RCMs) from the latest version of Rossby Centre of Atmospheric models (RCA4) in the simulation of precipitation over Greater Horn of Africa (GHA) from 1951–2005. The evaluation was performed against observed data from the Climatic Research Unit (CRU) and Global Precipitation Climatology Centre (GPCC). Results for mean seasonal analyses demonstrate an underestimation of March–May (MAM) and June–September (JJAS) precipitation whilst October to December (OND) precipitation is overestimated. Further assessment on the annual scale depicts underestimation of rainfall. However, the west to east gradient representing heavier to lighter precipitation and bimodal patterns of the north to south rainfall band is well captured by most models. The models fairly reproduce precipitation variability over the southeast region as compared to the northwest parts of the study domain. The mean ensemble invariably outperforms the individual RCA4 models due to its minimal probability deviance in precipitation in each zone and throughout the GHA region. The overall evaluation shows weak correspondence of the model data with observed CRU based on statistical metrics. The top five performing models are: MIROC5, CSIRO, CM5A-MR, MPI-ESM-LR, and EC-EARTH. Large variations of model performance are noted from one model to model, and from one region to the other. The ensemble mean of the outperforming RCMs reproduces the rainfall climatology over study domain with reasonable skill and the findings of this study will be a base for the study of extreme floods/droughts events in the region.

1. Introduction

The response of climatic features to ongoing global warming has been marked by increment in the intensity and magnitude of extreme events in most parts of the world (IPCC, 2014; Alexander, 2016). Consequently, sharp decline in light precipitation events and wet spell length coupled with increase in dry days and dry spells continue to pose a threat to livelihoods of communities who are dependent on rainfall for livelihood (World Bank, 2012). This calls for continuous assessment of spatiotemporal climatic characteristics in a bid to infer the evolving trends for both hydrological cycles and energy balance across different regions (Hu et al., 2019).

Over the years, many studies have employed the Global Climate Models (GCMs) in the appraisal of global and regional climate patterns (Christensen et al., 1997; Maidment et al., 2015; Almazroui et al.,

2017a, 2017b; Ongoma et al., 2018). However, coarse spatial resolutions of the GCMs that are unable to capture the mesospheric processes and dynamics driving the occurrence of such physical processes have prompted the idea of employing high resolution and dynamically downscaled regional climate models (RCMs) (Pal et al., 2007; Wilby and Fowler, 2010; Giorgi and Gutowski, 2015). Presently, many institutions continue to use RCMs for varying applications in climate studies (IPCC, 2014)

The development of RCMs has contributed immensely to the understanding of climate processes including extreme precipitation patterns and future projections of temperature trends in many regions of the world (Nikulin et al., 2012; Jacob et al., 2014; Russo et al., 2015). This is attributed to a flagship project from the Coordinated Regional climate Downscaling Experiment Program (CORDEX, <https://www.cordex.org/>) through World Research Climate Program (WRCP) that

* Corresponding author.

E-mail address: tanguirong@nuist.edu.cn (G. Tan).

<https://doi.org/10.1016/j.atmosres.2019.104705>

Received 22 May 2019; Received in revised form 23 August 2019; Accepted 12 October 2019

Available online 17 October 2019

0169-8095/© 2019 The Authors. Published by Elsevier B.V. This is an open access article under the CC BY license

(<http://creativecommons.org/licenses/by/4.0/>).

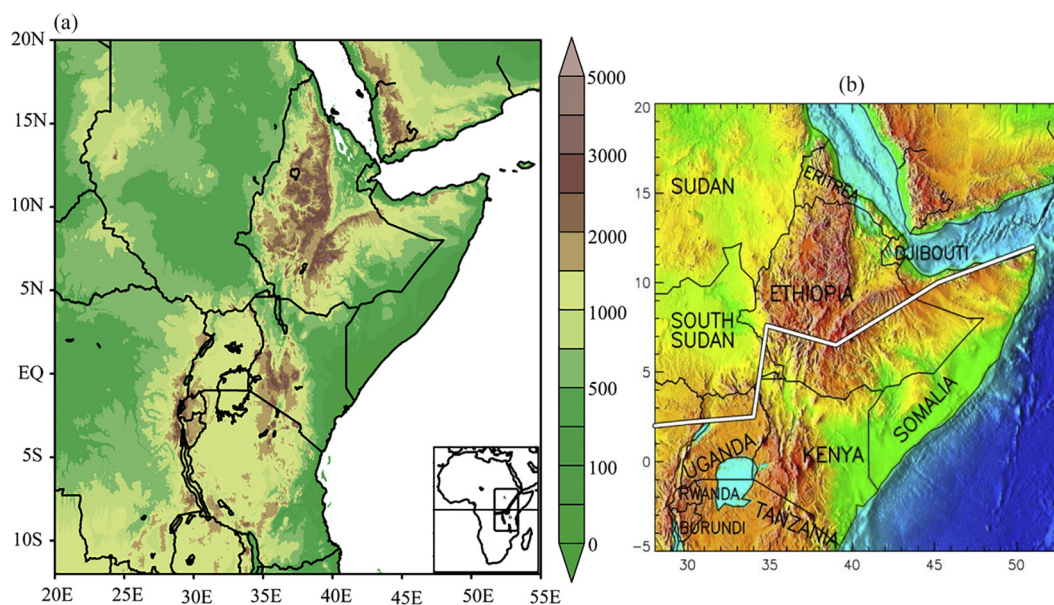


Fig. 1. a Map of the study area showing the location of Eastern African with enclosed African continent map. Fig. 1b (Nicholson, 2017) show the zone A represented in the northern sector ($5^{\circ}\text{N} - 20^{\circ}\text{N}$, $30^{\circ}\text{E} - 51.39^{\circ}\text{E}$) and the southern sector defined by equatorial rainfall regime as zone B ($12^{\circ}\text{S} - 4^{\circ}\text{N}$, $28^{\circ}\text{E} - 42^{\circ}\text{E}$). The white line superimposed upon the schematic diagram separates the zone A and B respectively.

dynamically downscaled GCMs to a high-resolution climate models available for end users (Giorgi et al., 2009).

Whereas improved performances have been reported in many regions that have employed RCMs, studies over conducted over Africa have reported the need for in depth evaluations to ascertain limitations of various models that could arise due different parameterizations employed or lateral boundary conditions (Gbobaniyi et al., 2013; Endris et al., 2013; Akinsanola et al., 2015). Christensen et al. (1997) reported the drawbacks of RCMs in their inability to improve the systematic errors arising from large-scale circulations that are used as driving models.

Over East Africa, a number of studies have evaluated the existing RCMs in order to ascertain their performance (Indeje et al., 2000; Anyah et al., 2006; Segele et al., 2009; Diro and Tompkins, 2012; Endris et al., 2013, 2015; Luhunga et al., 2016; Osima et al., 2018). This trend is observed in other regions across African. For instance, west Africa (Diallo et al., 2012; Sylla et al., 2013; Akinsanola et al., 2015; Klutse et al., 2016), central Africa (Haensler et al., 2013; Vondou and Haensler, 2017; Fotso-Nguemo et al., 2017), south Africa (Favre et al., 2015; Kalognomou et al., 2013; Pinto et al., 2015; Maure et al., 2018), Arabian Peninsula (Almazroui, 2019), and north Africa (Tramblay et al., 2013).

Majority of these studies were however, based on the first phase of the CORDEX where most model centers employed ERA Interim reanalysis (Dee et al., 2011) as driven runs (Akinsanola et al., 2017). The second phase entail GCMs that participated in Coupled Modelling Intercomparison Project (CMIP5) (Taylor et al., 2012) for downscaling the historical run and future climate projections. An example is the latest version of regional climate model (RCA4) developed by the Swedish Meteorological and Hydrological Institute (SMHI) (Samuelsson et al., 2012). The RCA4 model is advanced from High Resolution Limited Area Model (HIRLAM; Unden et al., 2002), which is a numerical weather prediction (NWP) forecasting system, resulting into enhanced physical and dynamical parameterization (Strandberg et al., 2014; Tamoffo et al., 2019).

Few studies have evaluated such recent developments in RCMs over EA region (Luhunga et al., 2016; Souverijns et al., 2016; Mutayoba and Kashaigili, 2017; Osima et al., 2018). Endris et al. (2013) performed an overall assessment of ten RCMs over GHA region. The study employed daily data including the old version of RCA35. The report noted some

wet biases during the summer rainfall over northwest sides of study domain as well as the eastern sides. Over Uganda, Kisembe et al. (2018) observed the impuissance of the models to reproduce ‘short’ and ‘long’ rains despite the positive mode of El Nino Southern Oscillation (ENSO) or Indian Ocean Dipole (IOD).

Although, most studies have reported a reasonable performance of mean ensemble of RCMs in reproducing the annual cycle, trends and inter-annual variability of climate features over the study domain, the individual models still exhibit potential uncertainties that needs to be improved before the datasets can be employed for climate change impact analysis over the study region. Stensrud (2007) points out a number of factors contributing to model error over the study domain among them being convective parameterization and limited resolutions driving boundary models.

The aim of this study is to assess the performance of the latest version of monthly RCMs simulations that were dynamically downscaled from CMIP5 GCMs by Rossby Centre Regional Climate Models (RCA4), developed by SMHI under CORDEX-Africa. With advent of extreme events that continue to affect the region characterized by increase (decrease) in drought (rainfall), understanding the performance of the best model will be significant in exploring the projected changes for planning purposes. The coverage of the remaining sections in this paper is as follows: Section two highlights study area, datasets employed and methods whereas third section gives the findings and the corresponding discussions. Lastly, conclusion and recommendation are presented in Section 4.

2. Data and methodology

2.1. Locality of study

The GHA covers: Burundi, Djibouti, Ethiopia, Eritrea, Kenya, Rwanda, Tanzania, Somalia, South Sudan, Sudan, and Uganda (Fig. 1). The domain is located astride the equator lying within $11.74^{\circ}\text{S} - 20^{\circ}\text{N}$, and $21.84^{\circ}\text{E} - 51.39^{\circ}\text{E}$. In this study, the area was further divided into two main zones: northern section defined characteristically by summer rainfall as **Zone A** ($5^{\circ}\text{N} - 20^{\circ}\text{N}$, $30^{\circ}\text{E} - 51.39^{\circ}\text{E}$) and the southern section defined by equatorial rainfall regime as **Zone B** ($12^{\circ}\text{S} - 4^{\circ}\text{N}$, $28^{\circ}\text{E} - 42^{\circ}\text{E}$) (Fig. 1b; Nicholson, 2017). These zones are identified following the earlier studies that categorized whole Africa into fifteen

unvarying sub regions (Indeje et al., 2000; Indeje and Semazzi, 2000) who categorized regions superimposed upon intricate geomorphology. The varying elevation of the region influence local circulation, by enhancing the buoyancy which results in local precipitation (Mukabana and Pielke, 1996; Indeje et al., 2000, Indeje and Semazzi, 2000; Camberlin and Okoola, 2003; Oettli and Camberlin, 2005; Ogwang et al., 2014).

The climate of the study region classified as tropical climate is characterized by dry climate anomaly despite being located in equatorial belt. The rainfall patterns are highly heterogeneous, influenced by a number of factors over space and time. Zone B of the region is characterized by two rainy seasons, MAM and OND (Maidment et al., 2015; Ayugi et al., 2016, 2019; Ongoma and Chen, 2017) whereas Zone A experiences rainfall gradient during local summer of June to September (JJAS). The shifting of convective clouds belt, Inter Tropical Convergence Zone (ITCZ) is characterized by shift in the wind direction, from a northerly direction during December to February season and southerly direction during boreal summer impacting largely on the wet seasons observed (Nicholson, 2008; Hastenrath et al., 2011).

2.2. Data

2.2.1. Reanalysis datasets

Limited quality of observed data is still a challenge in evaluation of model simulations across Africa (Nikulin et al., 2012; Endris et al., 2013). To overcome this obstacle, this study used two observed reanalysis monthly datasets to evaluate the RCA4 simulations. The Climatic Research Unit (CRU TS v4.02) precipitation dataset with a 0.5° x 0.5° resolution (Harris et al., 2014) and the latest version of the Global Precipitation Climatology Centre (GPCC v8) of similar resolution were employed. The two datasets reproduce the precipitation well, with CRU slightly outperforming GPCC (Ongoma and Chen, 2017).

2.2.2. Model datasets

This study employed monthly rainfall datasets from ten RCA4 simulations driven by GCMs from CMIP5. Table 1 presents a comprehensive list of the GCMs from CMIP5 datasets employed in the study. The CGCMs employed were processed based on deterministic approach of dynamical downscaling of recent version of RCA4 developed by the SMHI under the CORDEX infrastructure over diverse regions in the globe (Samuelsson et al., 2012; Strandberg et al., 2014). This study focused on simulations of rainfall over CORDEX-AFRICA domain (AFR-44: 0.44 degree ~50 km resolution). All the approximations datasets are acquired from Rossby Atmospheric Modelling Centre. The data is accessible through the Earth Systems Grid Federation (ESGF) under the CORDEX project (<https://www.smhi.se/en/research/research-departments/climate-research-rossby-centre2-552>). Moreover, a mean ensemble of the ten RCA4 simulations was equally evaluated. The precipitation estimates from the RCM data were provided in terms of flux (kg/m²s), whereas the observed estimates were provided in terms of monthly accumulated rainfall amount (mm/month). To address this

Table 1

The description of the Global Climate Models (GCMs) dynamically downscaled by RCA4 CORDEX.

Institute	GCM name	Abbreviated name
1. Canadian centre for climate modeling and analysis (Canada)	CCCma-CanESM2	CanESM2
2. Centre national de recherches météorologiques (France)	CNRM-CRAFACS-CNRM-CM5	CNRM-CM5
3. Met office hadley centre	MOHC-HadGEM2-ES	HadGEM2-ES
4. Consortium of european research institution and researchers	ICHEC-EC-EARTH	EC-EARTH
5. NOAA geophysical fluid dynamics laboratory, USA	NOAA-GFDL-GFDL-ESM2M	GFDL-ESM2M
6. Institut pierre-simon laplace, France	IPSL-IPSL-CM5A-MR	IPSL-CM5A-MR
7. National institute for environmental studies, and japan agency for marine-earth science and technology (MIROC), Japan	MIROC-MIROC5	MIROC5
8. Commonwealth scientific and industrial research organization	CSIRO-MK3-6-0	CSIRO
9. Max planck institute for meteorology (Germany)	MPI-M-MPI-ESM-LR	MPI-ESM-LR
10. Norwegian climate centre (Norway)	NCC-NorESM1-M	NorESM1-M

problem, precipitation flux was converted into monthly accumulated rainfall using every month's data matrix (Eq. (1));

$$T_{mm/month} = n_{s/min} \times n_{min/h} \times n_{h/day} \times n_{day/month} \times F_{kg/m2s} \quad (1)$$

where $T_{mm/month}$ is the considered month's data matrix in mm/month, $n_{s/min}$ is the number of seconds per minutes, $n_{min/h}$ is the number of minutes per hour, $n_{h/day}$ is the number of hours per day, $n_{day/month}$ is the number of days in the considered month, and $F_{kg/m2s}$ is the considered month's original precipitation flux data matrix.

2.3. Methodology

The study employed various scalar accuracy measures to evaluate RCA4 in reproducing the fundamental characteristics of precipitation for the period 1951–2005 over GHA. Three rainfall seasons (JJAS for Zone A, and MAM and the OND for Zone B) were identified for comparative analysis in two distinct zones of the study domain. The study used mean seasonal, annual and inter-annual variations as a way of assessing the skillful simulation of rainfall over the region. In addition, a detailed statistical evaluation was employed to compare the model's performance. They include correlation coefficient (CC), bias (B), and root mean square error (RMSE), amongst the reanalysis and simulated rainfall cycle by the RCA4 models. The mathematical formulas of the metrics employed are as shown in Eqs. (2)–(4):

$$B = \frac{1}{N} \sum_{k=1}^N (M_i - O_i) \quad (2)$$

$$CC = \frac{\sum_{k=1}^n (O_i - \bar{O}_i)(M_i - \bar{M}_i)}{\sqrt{\sum_{k=1}^n (O_i - \bar{O}_i)^2 \sum_{k=1}^n (M_i - \bar{M}_i)^2}} \quad (3)$$

$$RMSE = \sqrt{\frac{1}{N} \sum_{k=1}^N (M_i - O_i)^2} \quad (4)$$

where M and O are the model simulated and observed values, respectively. I refers to the simulated and observed pairs and N is the total number of such pairs being evaluated. Further details concerning the employed statistical metrics are available on previous studies (Wilks, 2006; Dinku et al., 2009; Segele et al., 2009; Ongoma et al., 2019). Moreover, the Mann-Kendall (MK; Mann, 1945; Kendall, 1975) test was performed to detect trend. In addition, a cumulative frequency distribution (ECDFs) for all the models runs were compared with that of observed datasets to determine the symmetries of simulations deviating from the observed patterns. The ECDFs employed to fit different theoretical distributions of the models against the observed as previously used by Akinsanola et al. (2017).

3. Results and discussion

3.1. Seasonal climatology

First, the ability of RCA4 datasets to reproduce mean seasonal

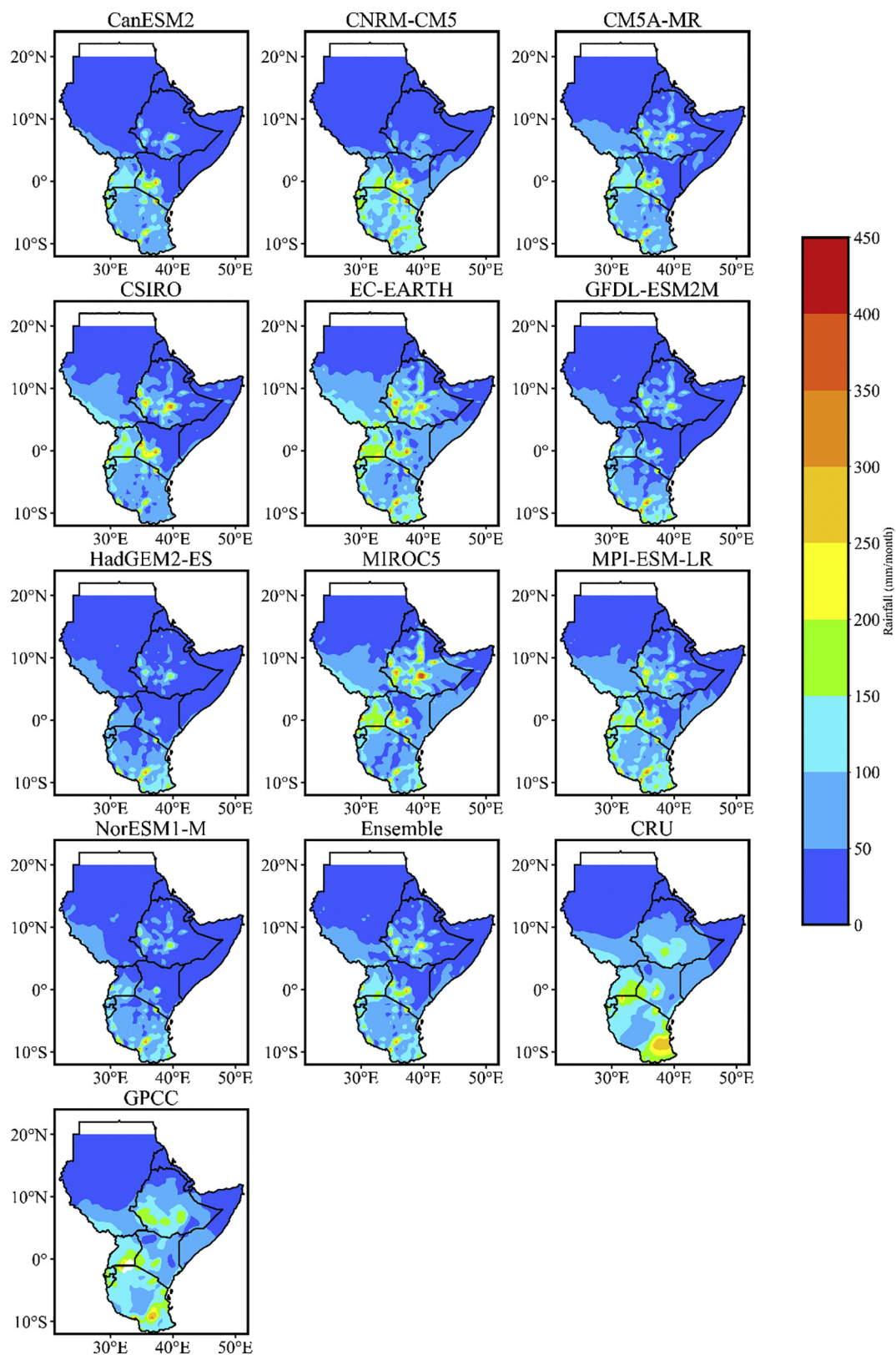


Fig. 2. Spatial distribution of MAM mean rainfall (mm/month) over Eastern Africa from 1951 to 2005 for (a) GPCC, (b) CRU (c) CanESM2, (d) CNRM-CM5, (e) CSIRO, (f) ECEARTH, (g) IPSL-CM5A-MR, (h) HadGEM2-ES, (i) MPI-ESM-LR, (j) NorESM1-M, (k) GFDL-ESM2M, (l) MIROC5, and (m) ENSEMBLE.

climatology of monthly precipitation characteristics over GHA was assessed. The spatial patterns of mean March to May (MAM) is presented in Fig. 2 where RCA4 models, together with the mean ensemble are assessed against CRU and GPCC. Further, OND over Zone B and summer

rainfall (JJAS) over Zone A are presented in Figs. 3 and 4, respectively. The RCA4 rainfall simulations are consistent with observed datasets: GPCC and CRU in all the seasons. It is evident that the regional mesospheric features and the north-south oscillation of the ITCZ that have

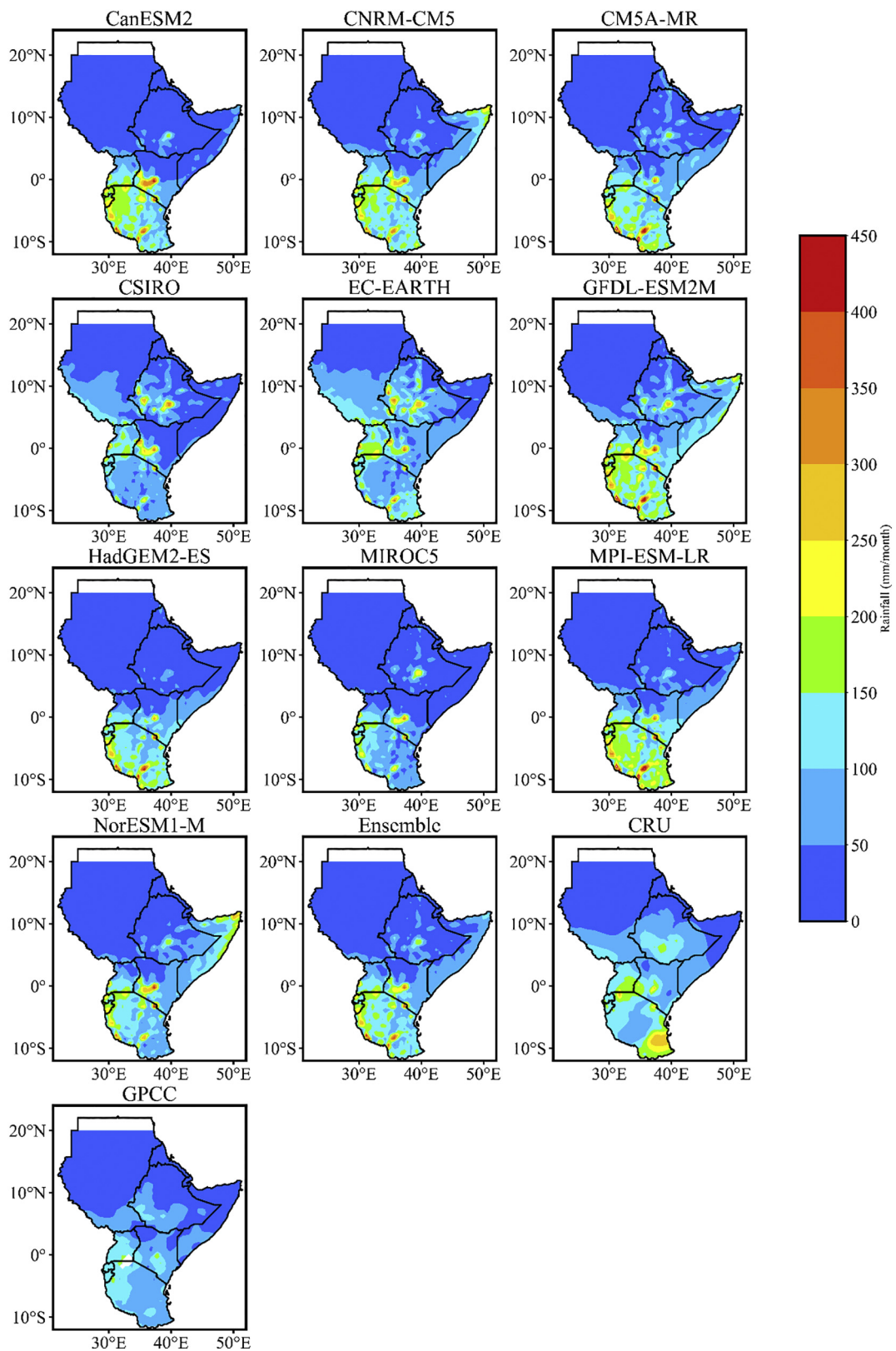


Fig. 3. Same as Fig. 2 but for OND.

considerable influence on the distribution of rainfall (Nicholson and Kim, 1997) are well captured by most models.

In MAM season, most models except for HadGEM2-ES, GFDL-ESM2M, and NorESM1-M captured west to east slope (Fig. 2). This symbolizes significant to low rainfall events. The highest seasonal

rainfall amount recorded was 1800 mm whilst the least amount of rainfall recorded has a measure of about 810 mm/month. Moreover, the RCA4 products of CM5A-MR, HadGEM2-ES, and NorESM1-M poorly capture the simulated rainfall over northwest Ethiopian highlands and Nile valley basin. The western sides of the study area are characterized

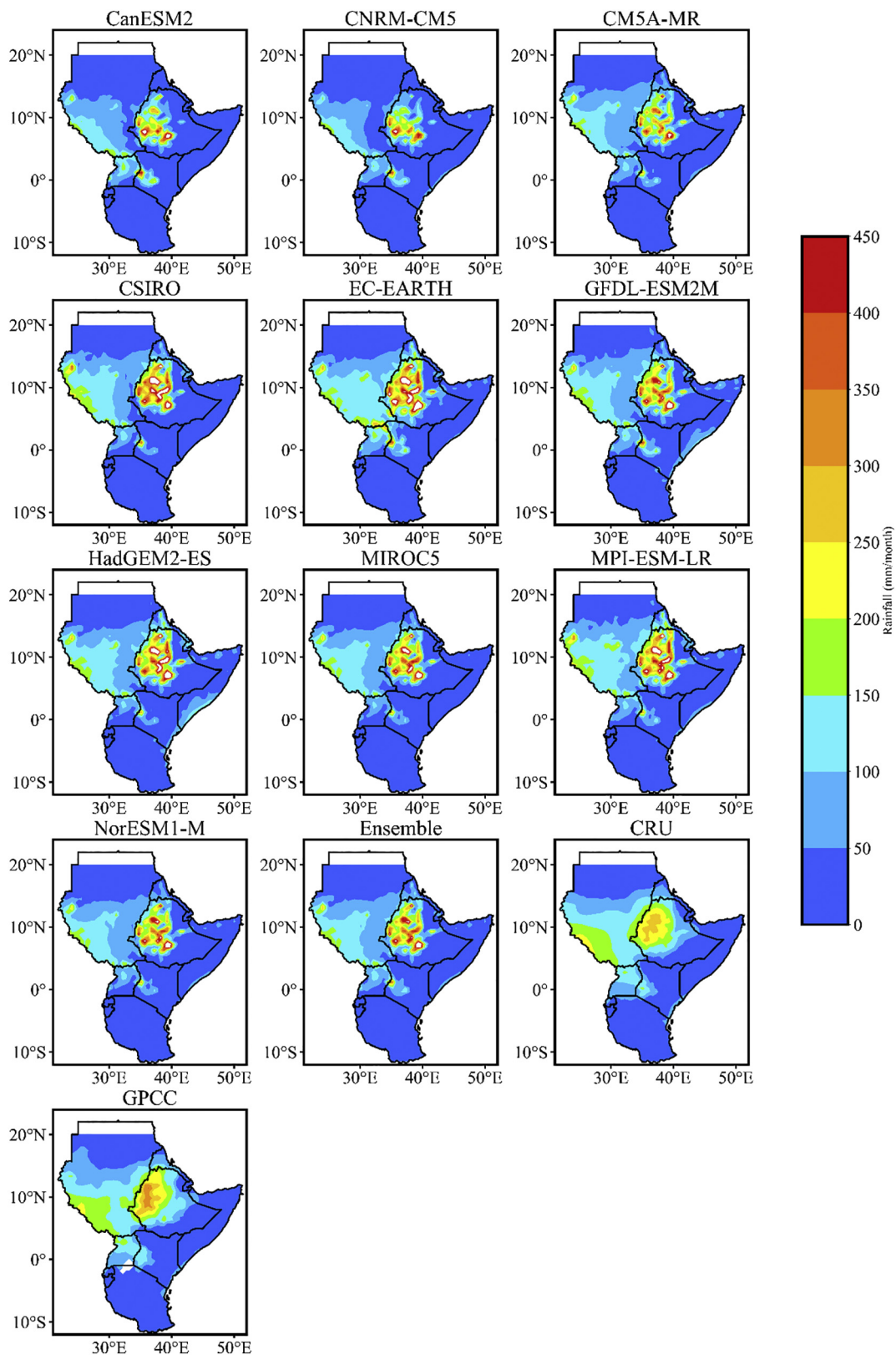


Fig. 4. Same as Fig. 2 but for JJAS.

by complex topography and presence of large water bodies modulating convective features. The models that perform relatively in MAM season are: EC-EARTH, MIROC5, MPI-ESM-LR, and mean ENSEMBLE. This agrees with past studies that observed the changes in season coinciding with the location of rainfall band over the GHA domain (Endris et al.,

2013; Souverijns et al., 2016).

During the OND, most RCA4 models reproduce the precipitation patterns depicting heavier concentration of rainfall band over western sides along the equator as compared to the eastern gradient (Fig. 3). Most models overestimate the rainfall amount observed except for

MIROC5, CSIRO, and CanESM2. The GFDL-ESM2M highly overestimate the observed rainfall during OND season as compared to all other models. The observed overestimation by mean ENSEMBLE data points to the fact that RCA models capture the increase in precipitation despite underestimation recorded by the models. For summer rainfall over the Zone A domain, the mean precipitation shows similar pattern as observed by CRU and GPCP (Fig. 4; JJAS). Interestingly, five models overestimated the observed CRU rainfall while the rest recorded underestimation of the observed precipitation. However, the GPCP had seven models underestimating the observed precipitation whilst four noted an overestimation of the same. Relatively higher precipitation is observed in the northern parts of Ethiopian highlands than Sudan plain terrains. Mean precipitation amount is relatively consistent in all RCA4 products as compared to large scale differences in observed mean summer precipitation. The GFDL-ESM2M, EC-EARTH and MPI-ESM-LR demonstrated similar distribution as observed with overestimation reported, whereas CM5A and CanESM2 show inconsistent spatial patterns and underestimation performance. Essentially, most studies based on RCMs or GCMs have reported projected wetting over the study area (Shongwe et al., 2011; Kent et al., 2015; Ongoma et al., 2018).

From the seasonal climatology, it can be deduced that RCA4 precipitation products consistently present spatial variations of rainfall over the study domain. A precipitation pattern over GHA is diverse and hence small deviation in terms of relatively high rainfall can be observed for different products. All RCA4 products were able to reproduce the seasonal and spatial variability over the study region with maximum amount of rainfall values recorded during summer rainfall and OND season. However, MAM season presented reasonably agreeable values as observed based on reanalysis datasets. The large-scale and local dynamics (Nicholson and Kim, 1997; Saji et al., 1999; Indeje et al., 2000) governing the precipitation variability over study area are all presented in the models' datasets, despite the slight deviation in regards to mean values. Thus, most model underestimate MAM and JJAS while overestimation is noted during OND rainfall across the study domain.

3.2. Annual cycle

The annual cycle of monthly precipitation averaged over two sub-equatorial regions are presented in Fig. 5 and Table 2. It is apparent that model datasets capture prominent features of the annual rainfall patterns associated with the oscillation of the ITCZ. The convergence of the ITCZ leads to increased moisture flux from easterly and westerly flow during the peak seasons as represented by models and observed datasets. The low-pressure belt, characterized by convective activities that enhances precipitation amount often migrates from 15° S to 15° N between January and July (Camberlin and Wairoto, 1997). This results in a bimodal pattern (MAM and OND) over Zone B whereas single boreal summer peak (JJAS) is experienced in Zone A. However, the models underestimate annual rainfall over the region despite the small values of RMSE indicating minimal biases in the spatial patterns of the mean annual rainfall (Table 2).

On the contrary, most models poorly presented the OND peaks with overestimations observed except for MIROC5 and CSIRO. This agrees with the recent study by Endris et al. (2013) that reported similar patterns where RCMs models poorly reproduced the OND peak. The EC-EARTH model overestimated precipitation in all regions by 68 mm/year for Zone A and 80 mm/year for Zone B whilst CanESM2 strongly underestimated the annual cycles in Zone A (Table 2). Similar performance of the EC-EARTH model is observed in Central Africa (Fotso-Nguemo et al., 2017). The RCA4 models performance of underestimation (overestimation) of annual rainfall cycle concur with the findings of the past studies carried out in different places over Africa (Kalognomou et al., 2013; Luhunga et al., 2016; Mutayoba and Kashaigili, 2017; Akinsanola et al., 2017; Kiembe et al., 2018; Warnatzsch and Reay, 2019).

Despite the ENSEMBLE mean's underestimation of precipitation

between 74 and 101 mm/year in all regions, it outperforms individual models. These observations exemplify the need to primarily, identify suitable models over diverse heterogeneous climatic zones in GHA region that precisely estimate rainfall amounts. The need for accurate datasets that can clearly represent the climatic variations in the advent of increase in extreme events is long overdue in the region that is overly depend on rainfall for agricultural production. Underestimation (overestimation) of long (short) rains continues to cause anxiety in a region whose climate is termed as a 'paradox', owing to uncertainty in the future of rainfall vis-a-vis the observed.

3.3. Interannual variability

Figs. 6 and 7 illustrate the interannual variability of standardized precipitation anomalies over the GHA sub-regions from 1951 to 2005. The anomalies are calculated with respect to the precipitation mean derived from the full study period. The results for interannual variability of annual precipitation anomalies for CRU and GPCP show a good agreement over Zone B as compared to Zone A with high correlation coefficient of 0.98 while for Zone A is 0.75. The majority of the RCMs fail to reproduce the year-to-year variations of the precipitations anomalies illustrating the difficulty to properly simulate fluctuations in the factors controlling interannual variability of precipitation over GHA. As for the seasonal rainfall anomalies of the RCMs and their respective ensembles over similar sub-regions of GHA, Endris et al. (2013) reported a realistic performance by the RCMs over the eastern region as compared to the northwest in simulating interannual variability of precipitation. On the other hand, Kiembe et al. (2018) noted better performance of RCMs in reproducing the interannual variability of the dry season but fail during rainfall seasons (MAM and OND) even if the ENSO and IOD signal is correctly simulated with most models. Meanwhile, multi-model mean ensemble depicted unsatisfactory performance in both regions, with unrealistic patterns over Zone A. The CanESM2, CM5A-MR, NorESM1-M, and GFDL-ESM2M show high amplitudes as compared to observed data in Zone A. In both sub-regions, the mean ENSEMBLE showed relatively better performance over Zone B as compared to individual models.

Assessing the models' accuracy in simulating the interannual variability provides essential insights on the key drivers of relative changes in climate over a particular region. This is because large-scale factors influence the interannual variability of precipitation in most regions. For instance, over the GHA domain, factors such as seasonal amplitude of the Madden-Julian Oscillation (MJO), Indian Ocean SST, ENSO, monsoon winds, quasi-biennial oscillation (QBO), and IOD have been observed to have significant influence on interannual rainfall variability (Indeje et al., 2000; Hastenrath et al., 2011; Manatsa et al., 2014; Ogwang et al., 2015).

These variables are related with extraordinary precipitation that lead to flooding or dry conditions over the region (Camberlin and Okoola, 2003). Pohl and Camberlin (2006) noted the influence of MJO on occurrence of weather extremes characterized by anomalous wet or dry situations. However, studies (Black et al., 2003; Owiti et al., 2008) have ascertained strong variability occurs due to the changes in the Pacific Ocean and Indian Ocean circulations. For example, the years 1991, 1997, 2004 experienced below average rainfall whilst 1998, and 1999 received above normal rainfall, principally due to changes in ENSO activities. The extreme events are disastrous in the region. Thus, the capability of models to simulate observed climatic features provides an opportunity to identify the best possible models to be employed in studies and operations across the region. However, the unsatisfactory performance noted across the sub-regions in simulation of annual rainfall anomalies presents an opportunity for model developers to further improve the parameterization schemes in order to improve and have high skill model performance.

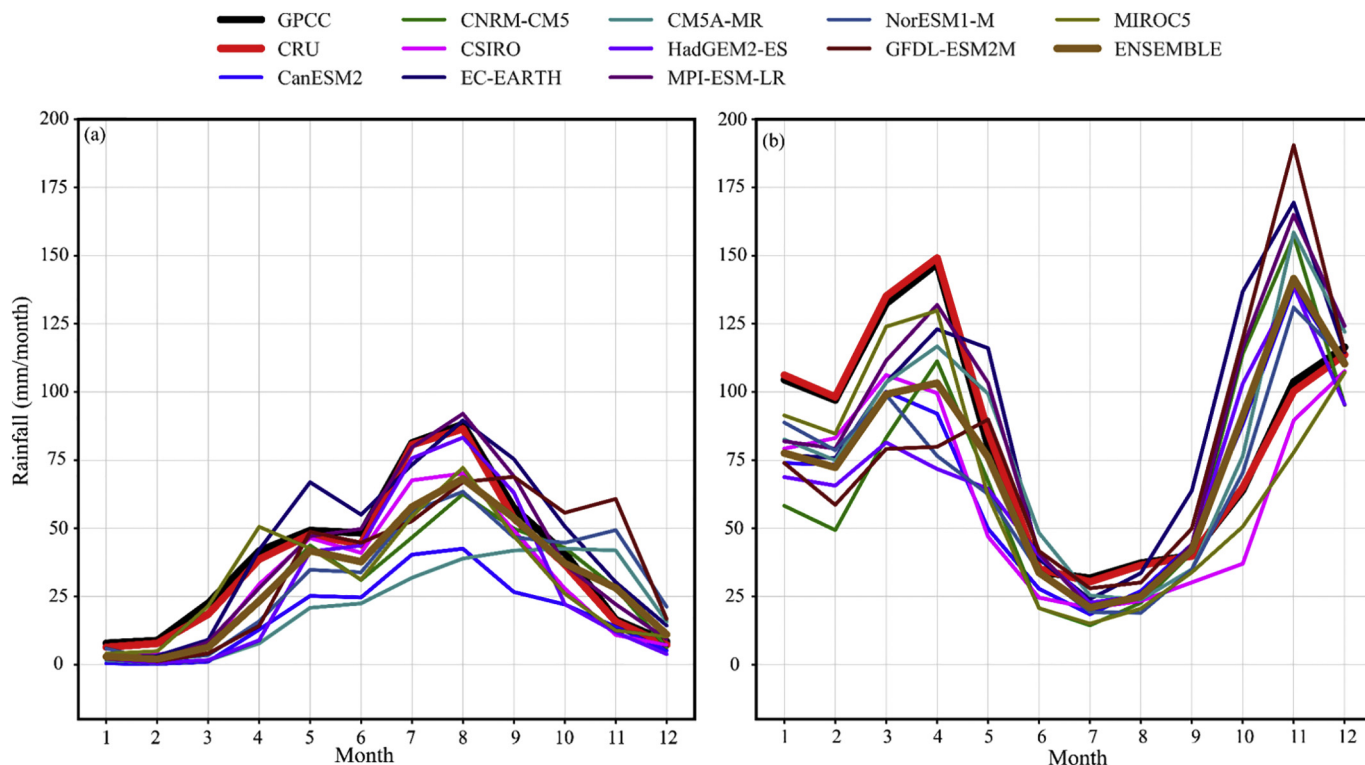


Fig. 5. Mean annual cycle of rainfall distribution during 1951-2010 over Eastern Africa region for regional models and observed datasets from (a) zone A and (b) zone B.

Table 2

Mean annual rainfall and the spatial RMSE (mm/month) with respect to CRU for models and ensemble over GHA region during 1951-2005.

Model data	Zone A		Zone B	
	Annual	RMSE	Annual	RMSE
CanESM2	215.28	23.22	842.99	28.4
CNRM-CM5	346.71	14.57	834.80	36.25
CSIRO	363.89	8.31	748.06	24.34
EC-EARTH	512.75	11.57	1076.27	34.86
IPSL-CM5A-MR	267.60	25.96	966.63	24.68
HadGEM2-ES	358.56	11.71	820.08	35.62
MPI-ESM-LR	446.09	7.17	1044.49	27.86
NorESM1-M	377.33	17.36	826.04	27.68
GFDL-ESM2M	438.82	19.84	956.05	42.69
MIROC5	377.63	10.92	817.41	15.63
ENSEMBLE	370.47	11.29	893.33	25.16
CRU	444.26	0.00	994.63	0.00
GPCC	471.30	0.00	988.46	0.00

3.4. Cumulative distribution function

Analysis obtained from the ECDFs of monthly precipitation is presented in Fig. 8. The ECDFs offer insight on the frequency of occurrence of precipitations on monthly basis over the region. Fig. 8a presents results of Zone A and demonstrates that most models slightly overestimate monthly precipitation (in range of 0 to 40 mm/month) over the region that experience dry climate anomalies. CanESM2 and CNRM-CM5 models undoubtedly overestimate the rainfall distribution whilst MIROC5, CSIRO and ENSEMBLE exhibit close amplitude from observed data in all values. On the contrary, the models EC-EARTH, MPI-ESM-LR, HadGEM2-ES, and GFDL-ESM2M underestimate the rainfall distribution between 20 and 60 mm/month.

The results for Zone B of RCA4 distribution with respect to observed data are shown in Fig. 8b. The performance of models over this region equally presents higher probabilities of large breadth relative to the

observed datasets. The ENSEMBLE mean shows consistent patterns despite some variations of overestimation of precipitation of more than 80 mm/month. Furthermore, CM5A-MR and MPI-ESM-LR exhibit similar close patterns as observed datasets. Most models overestimate the frequency with largest deviations depicted by HadGEM2-ES, CSIRO, CNRM-CM5, and CanESM2. Nevertheless, the models GFDL-ESM2M, EC-EARTH, and MPI-ESM-LR underestimate precipitation exceeding 100 mm/month.

The ENSEMBLE shows a consistent pattern with the observed datasets for the precipitation occurrence above 50 mm/month over the larger domain of GHA (Fig 8c). Most of the models overestimate the precipitation with pronounced amplitude as demonstrated in CanESM2 and CSIRO. The MIROC5, CNRM-CM5, and GFDL-ESM2M overestimated rainfall by < 50 mm/month and eventually underestimated heavier rainfall by > 60 mm/month. The EC-EARTH, HadGEM2-ES, and MPI-ESM-LR underestimate rainfall occurrence.

The results of these comparisons demonstrate that RCA4 models capture rainfall variations from one locale to another. The northwest region (Zone A) characterized by high altitude geomorphology exhibits overestimations of precipitation by CanESM2, CM5A-MR, and CNRM-CM5 whereas Zone B, with dominant plains and low plateaus bordering Indian Ocean display underestimations by GFDL-ESM2M, EC-EARTH and MPI-ESM-LR. The overall domain of GHA has the RCA4 underestimating rainfall with few models such as EC-EARTH exhibiting large amplitude of underestimations whilst CanESM2 showing contrary results. ENSEMBLE mean shows relatively good performance across all the diverse regions. This agrees with previous studies that reported improved performance Ensemble mean across diverse climatic zones in West Africa, based on daily datasets (Akinsanola et al., 2017).

3.5. Trend analysis

A brief of the annual and seasonal rainfall tendencies based on Mann-Kendall approach is presented in Table 3. The analysis was conducted over two distinct climatic zones as previously identified in a

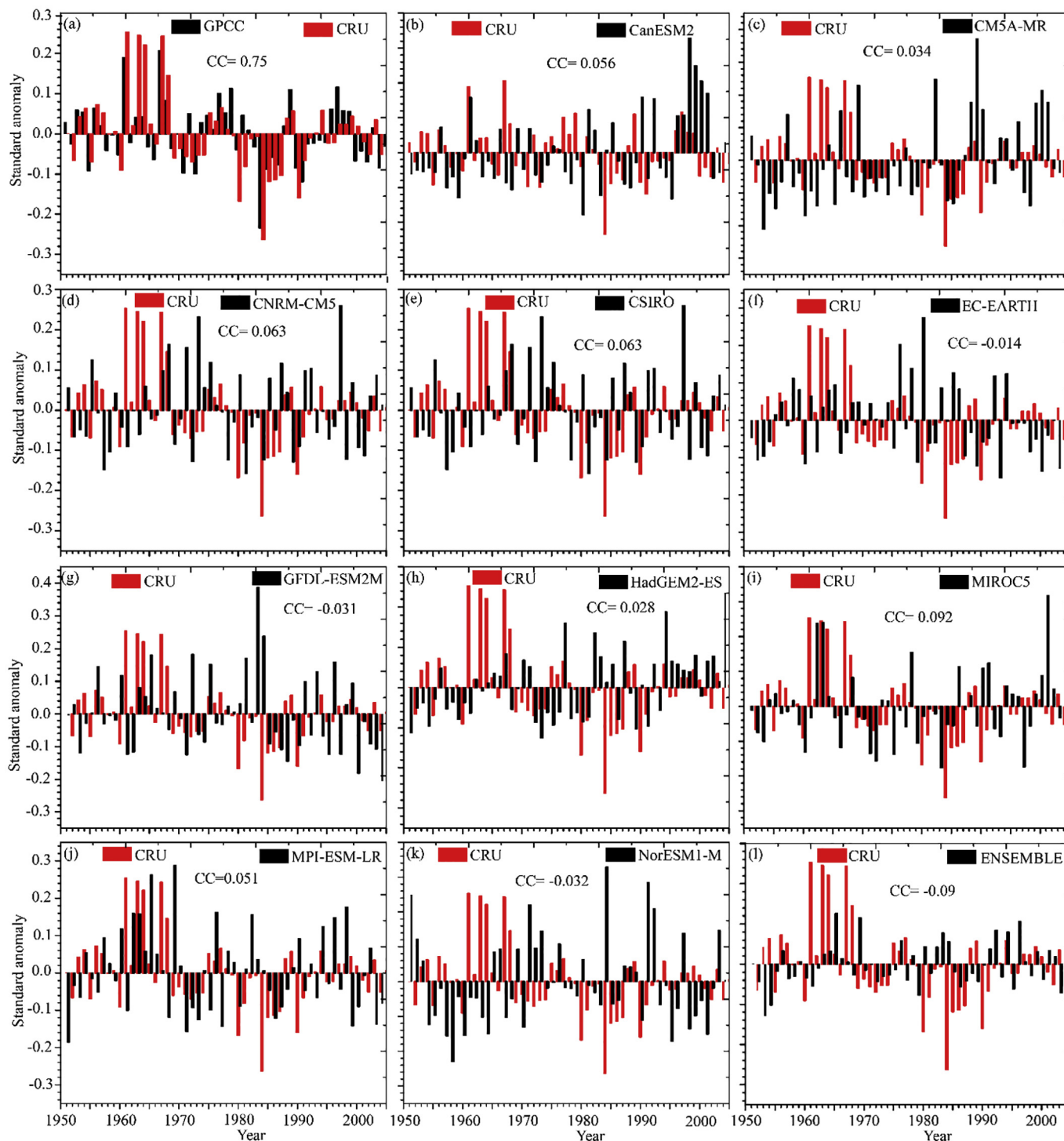


Fig. 6. Interannual variability of standardized precipitation anomalies over zone A of GHA for the period 1951-2005 for GPCCC and CRU; CRU and each RCMs and CRU; and the multi-model ensemble mean of anomalies.

study by Favre et al. (2011). The RCMs exhibit positive trends in annual rainfall over the two zones with models IPSL-CM5A-MR, MIROC5, HadGEM2-ES and ENSEMBLE demonstrating significant positive trends at 95% significant level over the Zone A.

At seasonal analyses, both the JJAS and local MAM rainfall exhibit significant decreasing trends as presented in the observed datasets whereas the OND shows increasing trends. The model IPSL-CM5A-MR particularly demonstrated a significant increasing trend of the OND while HadGEM2-ES did during the JJAS rainfall. The increasing trend of the local JJAS rainfall is in contrast to the observed pattern that

presented contrary tendencies. This finding agrees with the past studies that reported decreasing (increasing) trends in MAM (OND) over the GHA regions (Cook and Vizy, 2013; Liebmann et al., 2014; Ongoma and Chen, 2017). Funk et al. (2008) noted the decrease in the MAM rainfalls currently standing at 15% decline, is likely to continue on the downward trajectory owing to moisture deficits upstream catalyzed by the warming of Indian Ocean interrupting moisture transport.

The impact of the observed decline in rainfall is of great concern to society that is already food insecure coupled with growing population. In general, most models exhibit no significant trends over Zone B

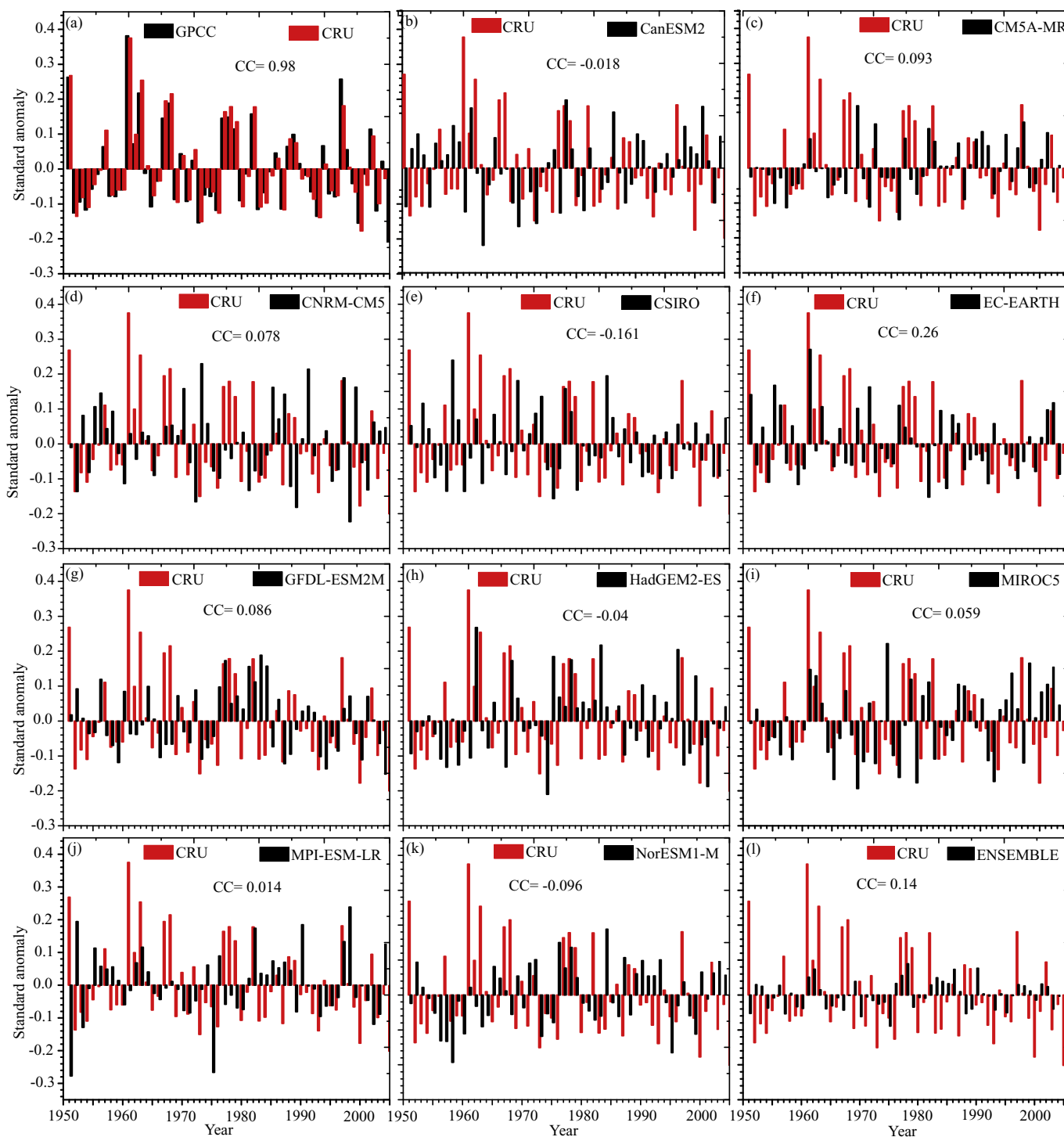


Fig. 7. Same as Fig. 6 but for zone B.

region. However, most of the RCA4 approximations were in agreement with the observations with slight difference in veracity level. The best models for annual and seasonal trend rainfall simulation are: IPSL-CM5A-MR, HadGEM2-ES, and the mean ENSEMBLE. Luhunga et al. (2016) in a study of RCMs CORDEX performance over Tanzania pointed that the observed tendencies in trends analysis of RCMs cannot be used to estimate model performance. For instance, the study reported decreasing trends that were characteristically non-statistically significant and hence could not demonstrate valuable information. Similarly, Mutayoba and Kashaigili (2017) concluded that RCMs forced by GCMs failed to simulate the trends in rainfall as compared to RCMs forced by

ERA-Interim reanalysis that fairly simulate trends in rainfall.

3.6. Statistical validation

A number of measurable measurements were employed to evaluate the RCA4 models capability in reproducing the rainfall climatology over the sub-regions of GHA domain. The results of the analysis are presented in Table 4. The suitability of the model performance presented in the analysis depicts overall weak CC, despite the low bias and RMSD. The GFDL-ESM2M show relatively better CC during MAM while MIROC5 reports fairly improved CC during JJAS. The highest reported

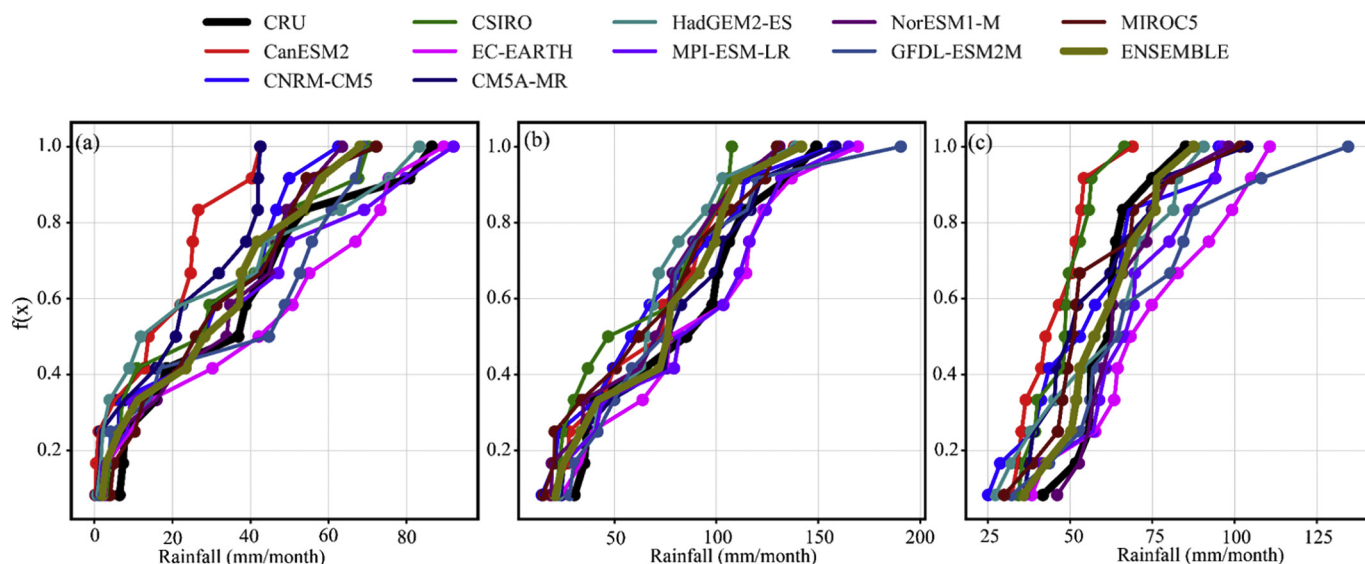


Fig 8. The cumulative distribution frequency of monthly mean precipitation amounts from the observed and model simulations for (a) Zone A, (b) Zone B, and (c) over whole GHA region during 1951-2005.

Table 3 Results of Mann-Kendall test over two distinct regions during 1951-2005.

Data	Zone A		Zone B		
	Annual	JJAS	Annual	MAM	OND
CRU	0.23	-0.02*	0.24	-0.03*	0.93
CanESM2	0.08	0.65	0.89	0.87	0.77
CNRM-CM5	0.69	0.73	0.46	0.72	0.95
CSIRO	0.87	0.64	0.71	0.94	0.91
EC-EARTH	0.39	0.26	0.36	0.26	0.85
IPSL-CM5A-MR	0.007*	0.88	0.15	0.74	0.01*
HadGEM2-ES	0.006*	0.02*	0.45	0.49	0.45
MPI-ESM-LR	0.33	0.78	0.36	0.26	0.42
NorESM1-M	0.57	0.66	0.13	0.11	0.53
GFDL-ESM2M	0.47	0.54	0.36	0.28	0.34
MIROC5	0.03*	0.26	0.11	0.08	0.20
ENSEMBLE	0.02*	0.37	0.65	0.09	0.41

Negative (positive) Z-values indicate decreasing (increasing) trend. The asterisk * stands for significant trend at 95% confidence interval.

correlation in this region among the RCA4 driven by GCMs from CMIP5 has a value of 0.23 as observed in GFDL-ESM2M. The short rain season over Zone B has MIROC5 and EC-EARTH exhibiting improved performance (CC=0.12). Similar performance of GFDL-ESM2M model before it was downscaled to RCM was reported in a study that evaluated CMIP5 rainfall simulations over the equatorial East Africa (Ongoma et al., 2019). Most importantly, the ENSEMBLE mean demonstrates noteworthy results during MAM as equated to each model runs as indicated. The findings show weak simulation of seasonal rainfall over this GHA region with Zone A indicating unsatisfactory performance with the observed datasets.

Further analyses of long-term variation of RCA4 and observed datasets were assessed spatially on interannual scale. The results show that HadGEM2-ES, CM5A-MR, MPI-ESM-LR, and ENSEMBLE have relatively high correlation, especially on the Zone A region as compared to Zone B (Fig. 9). The CC ranges from 0.4 to 0.8. On the contrary, EC-EARTH, GFDL-ESM2M, and NorESM1-M exhibited weak correlation (0.2 to 0.4) with the CRU data. Except for CSIRO and MIROC5, the rest of model demonstrated inconsistent performance over Zone B. This shows that most model dynamics for interannual precipitation is not agreeing to that of the observed datasets.

From Fig. 9, it is evident that RCA4 products are able to capture observed rainfall variability on interannual scale, especially on the

Table 4 A summary of the statistical comparisons between RCMs seasonal rainfall simulations and CRU datasets (mm/month) over GHA region during 1951-2005.

Seasons	Model	Bias	CC	RMSD	
MAM	CanESM2	-23.88	0.17	25.85	
	CNRM-CM5	-14.5	0.06	19.7	
	CSIRO	-14.41	-0.08	20.43	
	EC-EARTH	11.96	-0.23	17.38	
	IPSL-CM5A-MR	-11.64	-0.19	16.15	
	HadGEM2-ES	-21.1	0.02	25.19	
	MPI-ESM-LR	4.13	0.06	13.35	
	NorESM1-M	-6.98	-0.26	16.33	
	GFDL-ESM2M	-9.96	0.23	18.02	
	MIROC5	9.22	-0.10	15.24	
	ENSEMBLE	-7.79	-0.12	12	
	JJAS	CanESM2	-16.18	0.13	17.57
		CNRM-CM5	-3.74	-0.08	10.08
		CSIRO	-6.78	0.05	9.18
EC-EARTH		16.22	0.07	19.04	
IPSL-CM5A-MR		-11.49	-0.07	13.85	
HadGEM2-ES		15.35	0.15	17.9	
MPI-ESM-LR		8.87	-0.04	12.85	
NorESM1-M		1.91	-0.14	10.43	
GFDL-ESM2M		11.99	-0.01	18.34	
MIROC5		-13.11	0.21	14.6	
ENSEMBLE		0.3	0.06	5.33	
OND		CanESM2	-3.95	-0.11	14.02
		CNRM-CM5	17.95	-0.02	26.65
		CSIRO	-17.95	0.04	26.65
	EC-EARTH	28.04	0.12	35.32	
	IPSL-CM5A-MR	19.64	0	27.6	
	HadGEM2-ES	12.78	-0.03	24.28	
	MPI-ESM-LR	20.41	0.03	28.8	
	NorESM1-M	20.92	-0.02	30.99	
	GFDL-ESM2M	46.2	0.02	55.67	
	MIROC5	-7.59	0.12	15.75	
ENSEMBLE	13.71	0.06	18.29		

northern region. The strong airflow from Congo Basin and the mid tropospheric circulations from Atlantic Ocean (Nicholson, 2017) govern a dominant rainfall season in most parts of the Ethiopian highland and some parts of Sudan. A number of recent studies suggest the strong influence from Pacific and Indian Ocean in the annual contribution of rainfall totals (Nicholson and Selato, 2000; Williams et al., 2012). These rainfall systems were fairly reproduced by some models with variation in the 'CC' values that could be induced by land cover, climate

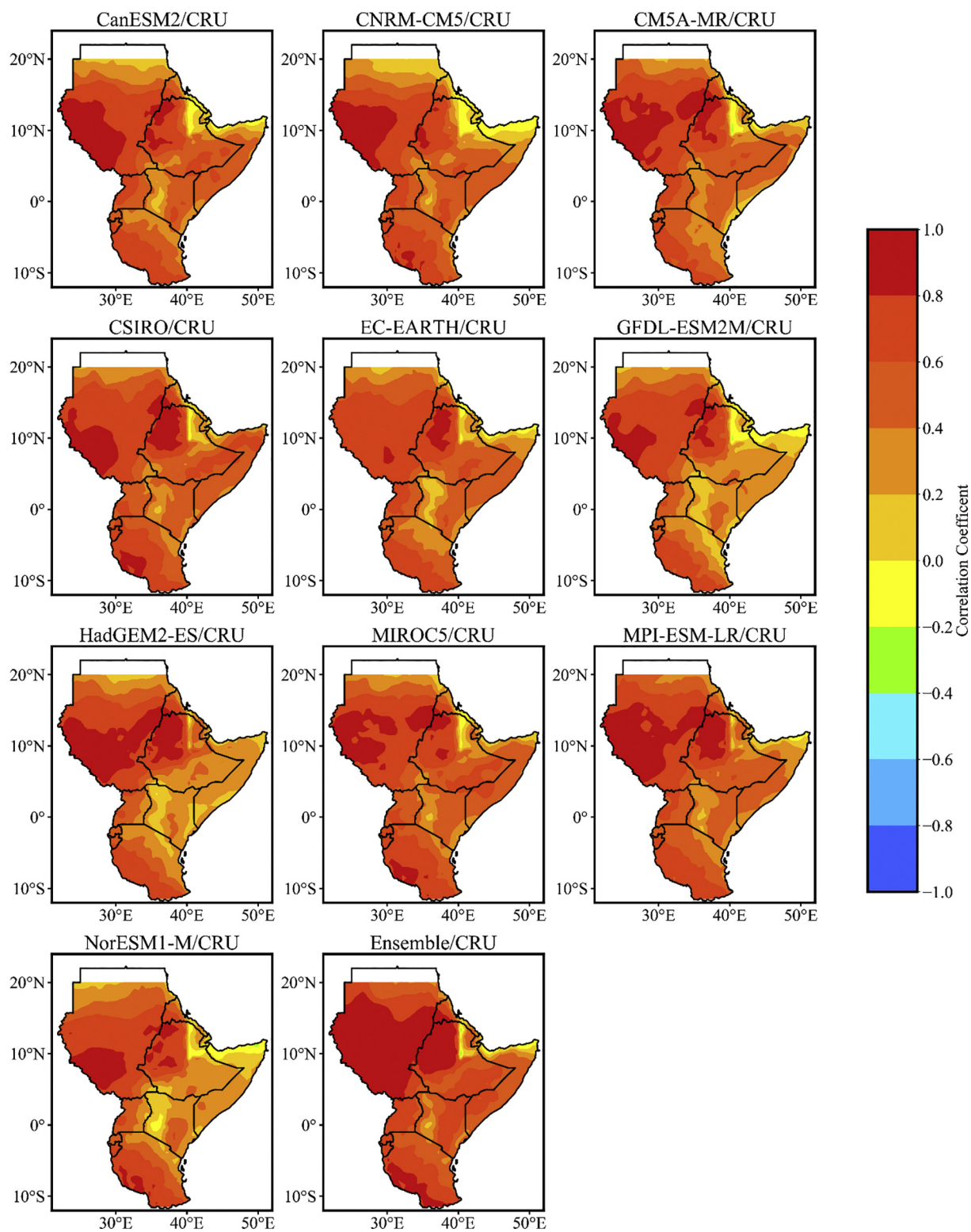


Fig. 9. Correlation coefficient of mean annual rainfall (mm/month) over Eastern Africa based on CRU datasets, 1951-2005.

conditions and terrain. Generally, precipitation varies in both time and space collation, with manifestation of different intensity and magnitude. Hence, the regions that exhibit low correlation could possibly be due to accuracy of observed data or different dynamics that resulted to associated uncertainties.

The RMSD of mean annual rainfall (mm/month) based on CRU datasets, 1951-2005, are shown in Fig. 10. The RMSD values indicate increase in southwards while a decrease in northern section of the study

domain indicating systematic differences in dynamics. The EC-EARTH, GFDL-ESM2M, and HadGEM2 exhibits RMSD values of > 100 to less than 250 mm in the southeast regions consistent in most locations with relatively higher altitude with wet climate. In east and north parts, characterized by ASALs terrain show low RMSD with significantly reduced low RMSD of 50 mm. The MIROC5 and ENSEMBLE mean depicted inconsistent performance with weak RMSD over most sections of the study domain. The GFDL-ESM2M showed agreement with, in most

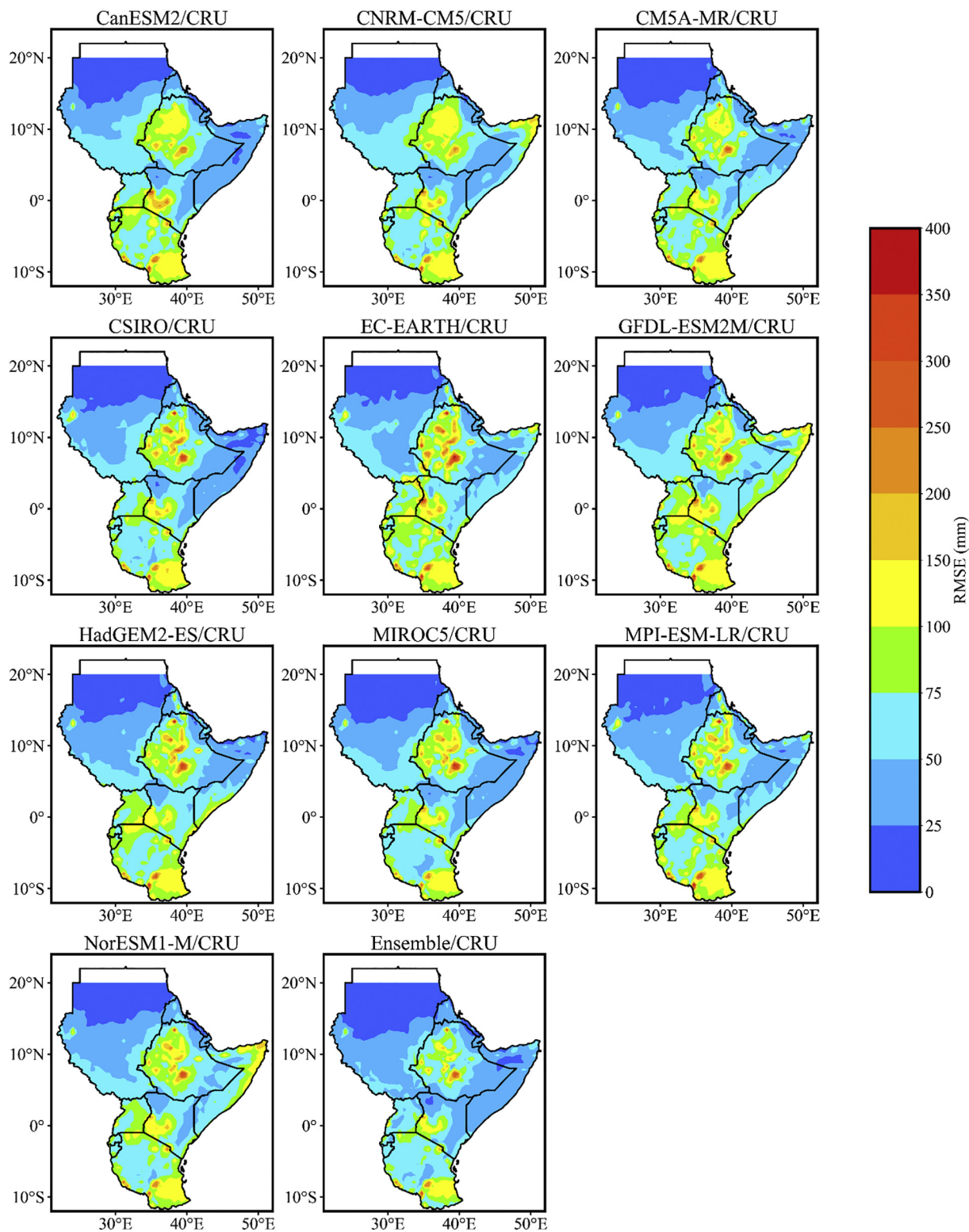


Fig. 10. RMSD of mean annual rainfall (mm/month) over Eastern Africa based on CRU datasets, 1951-2005.

parts of the region, high RMSD for regions around coastal belt, high altitude in central parts and over Ethiopian highlands. From the analyses in Fig. 10, it is clear that RMSD of most models vary in performance with variations to different climatic features and topography. High RMSD is observed in high altitude with wet climate regions whilst low RMSD is recorded in ASALs dry climate anomaly. Spatial plots of RCA4 products bias from the observed datasets for the GHA domain is

presented in Fig. 11. According to Endris et al. (2013), the model bias exhibits distinct variations and patterns from one model to another. However, CanESM2 and CNRM-CM5 show low bias over Zone A whereas HadGEM2-ES, CSIRO, and NorESM1-M exhibit weak bias in western belts around Uganda and lower regions of south Sudan. The systematic dry biases generally depicted over regions of low altitude characterized by ASAL climate maybe associated with moisture outflow

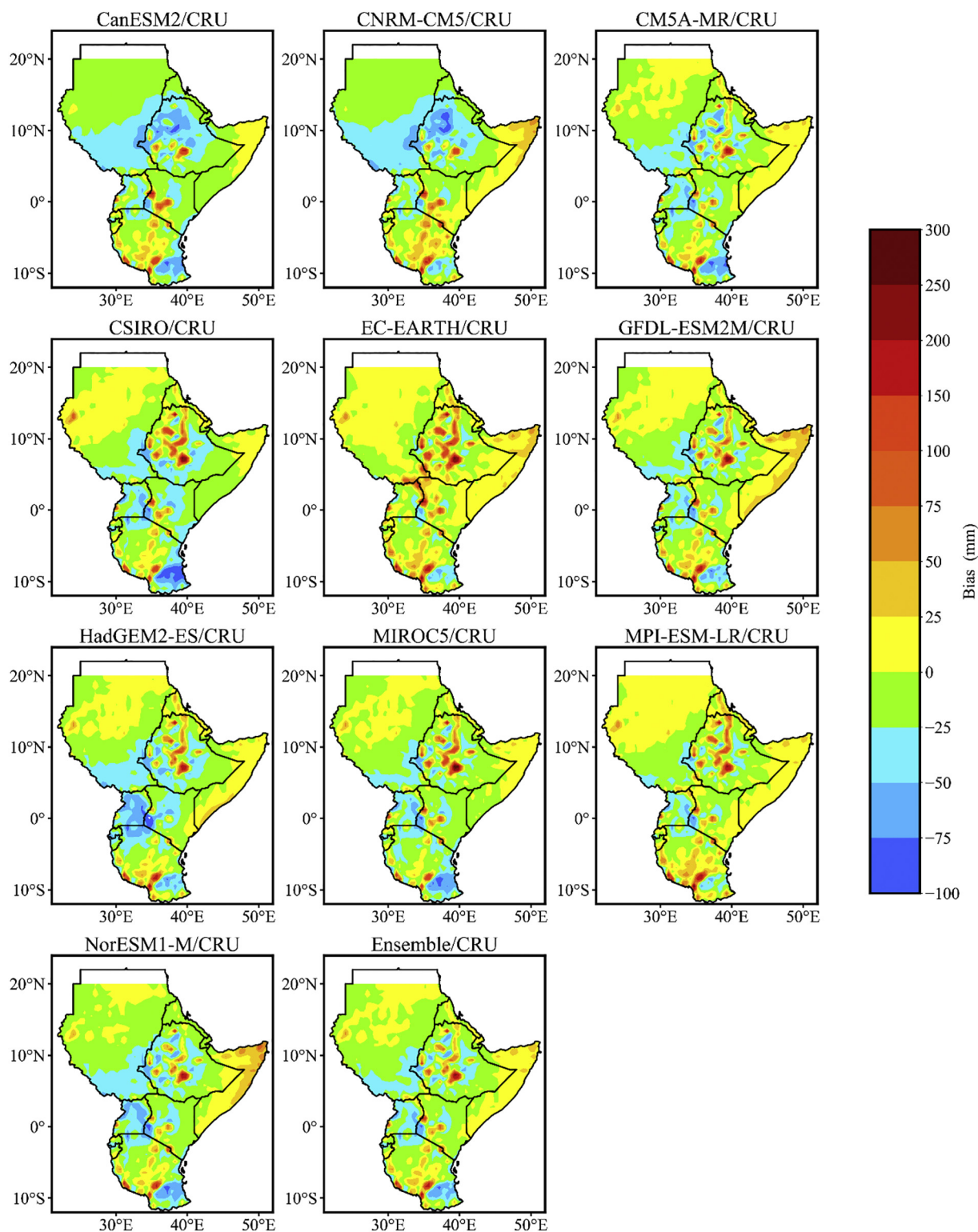


Fig. 11. Bias of mean annual rainfall (mm/month) over Eastern Africa based on CRU datasets, 1951-2005.

in this locales. Most mean spatial biases tends to follow the physiographic features in the study domain. For instance, the complex topography located over Zone A (Ethiopian highlands) and large mountains in Zone B, i.e. Mount Kenya, Mt. Kilimanjaro, Rwenzori ranges and Albertine Rift could not be clearly reproduced by RCMs due to coarser resolution and physical parameterization. This was noted by Favre et al. (2015) and Kisembe et al. (2018) over South Africa and Uganda, respectively.

In general, the statistical metrics of most models performance exhibit uncertainties over the study domain. The simulations are highly divergent across the models assessed in this study. Weak correlations between the RCA4 models and the observed data are not a constraint in the application of models for climate analysis. Furthermore, climate models may not depict specific weather event which may happen in a specific year, rather, they are utilized in the examination of climatic trends.

4. Conclusion and recommendation

In this study, RCA4 models have been evaluated for their capabilities to reproduce precipitation climatology during the period 1951–2005 over GHA. Findings from ten different RCMs developed by SMHI, namely the Rossby Centre regional atmospheric model (RCA4) with horizontal resolution of 0.44° are compared against two observed based reanalyzed datasets (GPCCv8 and CRU TS4.02). Performances of the RCA4 models together with the ensemble are evaluated at seasonal, annual, and inter-annual time lines. In addition, a number of statistical measurements are employed for robust analysis of the model performance. Results for mean seasonal analyses demonstrate an underestimation of March–May (MAM) and June–September (JJAS) seasonal precipitation whilst October to December (OND) precipitation is overestimated. Moreover, the west to east gradient representing heavier to low precipitation and bimodal patterns of north to south rainfall band is well captured by most models. Further assessment on the annual scale depicts underestimation of rainfall despite the small values of RMSE. During the long term simulation at inter-annual scale, majority of the RCMs fail to reproduce the year-to-year variations of the precipitations anomalies illustrating the difficulty to properly simulate fluctuations in the factors controlling interannual variability of precipitation over GHA. It is no doubt that the mean ensemble invariably outperforms the individual RCA4 models since it has minimal probability deviance in precipitation in each zone and over the whole GHA region. The overall evaluation shows weak correspondence with observed CRU based on statistical metrics. The better performing five models are: MIROC5, CSIRO, CM5A-MR, MPI-ESM-LR, and EC-EARTH. Large variations of model performance are noted from one model to another and from one region to the other. However, all the models present the bimodal patterns and the unimodal patterns over the two distinct regions assessed. The overestimations or underestimation of the models underscore the need to conduct bias corrections on the models outputs in order to rectify the systematic uncertainties before employing datasets for climate analysis application. The results in the present study offers insightful information on the CORDEX performance, in support of previous evaluative studies conducted over the study domain (Anyah et al., 2006; Endris et al., 2013). Therefore, the analysis elucidates the application of the ensemble of the recommended models for future climate projections and impact analysis in the ever increasing changes over the study domain.

Declaration of Competing Interest

All authors consent unanimously that there is no conflict of interest for this publication.

Acknowledgments

The authors acknowledge all model and reanalysis contributors for availing datasets to end users for possible analyses. Special acknowledgement go to Nanjing University of Information Science and Technology (NUIST) for setting up complimentary atmosphere and infrastructural needs for conducting research. National Key Research and Development Program of China (NKRDP; 2018YFC1505804) supported the study. In addition, National Natural Science Foundation of China (41575070 and 41430528) provided material facilitation. The lead author is grateful to NUIST for according him a PhD scholarship.

References

Akinsanola, A.A., Ogunjobi, K.O., Gbode, I.E., Ajayi, V.O., 2015. Assessing the capabilities of three regional climate models over CORDEX Africa in simulating West African summer monsoon precipitation. *Adv. Meteorol.* 2015, ID 935431. doi:<https://doi.org/10.1155/2015/935431>

Akinsanola, A.A., Ajayi, V.O., Adejare, A.T., Adeyeri, O.E., Gbode, I.E., Ogunjobi, K.O., Nikulin, G., Abolude, A.T., 2017. Evaluation of rainfall simulations over West Africa

in dynamically downscaled CMIP5 global circulation models. *Theor. Appl. Climatol.* 132 (1–2), 437–450. doi:<https://doi.org/10.1007/s00704-017-2087-8>.

Alexander, L.V., 2016. Global observed long-term changes in temperature and precipitation extremes: a review of progress and limitations in IPCC assessments and beyond. *Weather Clim. Extrem.* 11, 4–16. doi:<https://doi.org/10.1016/j.wace.2015.10.007>.

Almazroui, M., 2019. Temperature changes over the CORDEX-MENA domain in the 21st century using CMIP5 data downscaled with RegCM4: a focus on the Arabian Peninsula. *Adv. Meteorol.* doi:<https://doi.org/10.1155/2019/5395676>.

Almazroui, M., Nazrul Islam, M., Saeed, S., Alkhalaf, A.K., Dambul, R., 2017a. Assessment of uncertainties in projected temperature and precipitation over the Arabian Peninsula using three categories of Cmp5 multimodel ensembles. *Earth Syst. Environ.* doi:<https://doi.org/10.1007/s41748-017-0027-5>.

Almazroui, M., Saeed, S., Islam, M.N., Khalid, M.S., Alkhalaf, A.K., Dambul, R., 2017b. Correction to: assessment of uncertainties in projected temperature and precipitation over the Arabian Peninsula: a comparison between different categories of CMIP3 models. *Earth Syst. Environ.* doi:<https://doi.org/10.1007/s41748-017-0018-6>.

Anyah, R.O., Semazzi, F.H.M., Xie, L., 2006. Simulated physical mechanisms associated with climate variability over Lake Victoria in East Africa. *Mon. Weather Rev.* 134, 3588–3609. doi:<https://doi.org/10.1175/MWR3266.1>.

Ayugi, B.O., Wen, W., Chepkemoi, D., 2016. Analysis of spatial and temporal patterns of rainfall variations over Kenya. *J. Environ. Earth Sci.* 6 (11).

Ayugi, B., Tan, G., Ullah, W., Boiyio, R., Ongoma, V., 2019. Inter-comparison of remotely sensed precipitation datasets over Kenya during 1998–2016. *Atmos. Res.* 225 (1), 96–109. doi:<https://doi.org/10.1016/j.atmosres.2019.03.032>.

Black, E., Slingo, J.M., Sperber, K.R., 2003. An observational study of the relationship between excessively strong short rains in coastal East Africa and Indian Ocean SST. *Mon. Weather Rev.* 131, 74–94. doi:[https://doi.org/10.1175/1520-0493\(2003\)131<0074:AOSOTR>2.0.CO;2](https://doi.org/10.1175/1520-0493(2003)131<0074:AOSOTR>2.0.CO;2).

Camberlin, P., Okoola, R.E., 2003. The onset and cessation of the “long rains” in eastern Africa and their interannual variability. *Theor. Appl. Climatol.* 54 (1–2), 43–54. doi:<https://doi.org/10.1007/s00704-002-0721-5>.

Camberlin, P., Wairoto, J., 1997. Intraseasonal wind anomalies related to wet and dry spells during the “long” and “short” rainy seasons in Kenya. *Theor. Appl. Climatol.* 58, 57–69. doi:<https://doi.org/10.1007/BF00867432>.

Christensen, J.H., Machenauer, B., Jones, R.G., Schar, C., Ruti, P.M., Castro, M., Visconti, G., 1997. Validation of present day regional climate simulations over Europe: LAM simulations with observed boundary conditions. *Clim. Dyn.* 13 (7–8), 489–506. doi:<https://doi.org/10.1007/s003820050178>.

Cook, K.H., Vizy, E.K., 2013. Projected changes in east african rainy seasons. *J. Clim.* 26, 5931–5948. doi:<https://doi.org/10.1175/JCLI-D-12-00455.1>.

Dee, D.P., Uppala, S.M., Simmons, A.J., Berrisford, P., Poli, P., Kobayashi, S., Andrae, U., Balmaseda, M.A., Balsamo, G., Bauer, P., Bechtold, P., Beljaars, A.C.M., van de Berg, L., Bidlot, J., Bormann, N., Delsol, C., Dragani, R., Fuentes, M., Geer, A.J., Haimberger, L., Healy, S.B., Hersbach, H., Hólm, E.V., Isaksen, I., Kållberg, P., Köhler, M., Matricardi, M., McNally, A.P., Monge-Sanz, B.M., Morcrette, J.-J., Park, B.-K., Peubey, C., de Rosnay, P., Tavolato, C., Thépaut, J.-N., Vitart, F., 2011. The ERA-Interim reanalysis: configuration and performance of the data assimilation system. *Q. J. R. Meteorol. Soc.* 137 (656), 553–597. doi:<https://doi.org/10.1002/qj.828>.

Diallo, I., Sylla, M.B., Camara, M., Gaye, A.T., 2012. Interannual variability of rainfall and circulation features over the Sahel based on multipregional climate models simulations. *Theor. Appl. Climatol.* 113 (1–2), 351–362. doi:<https://doi.org/10.1007/s00704-012-0791-y>.

Dinku, T., Ceccato, P., Cressman, K., Connor, S.J., 2009. Evaluating detection skills of satellite rainfall estimates over desert locust recession regions. *J. Appl. Meteorol. Climatol.* 49 (6), 1322–1332. doi:<https://doi.org/10.1175/2010JAMC2281.1>.

Diro, G.T., Tompkins, A.M., Bi, X., 2012. Dynamical downscaling of ECMWF ensemble seasonal forecasts over East Africa with RegCM3. *J. Geophys. Res.* 117, D16103. doi:<https://doi.org/10.1029/2011JD016997>.

Endris, H.S., Omondi, P., Jain, S., Lennard, C., Hewitson, B., Chang’a, L., Awange, J.L., Dosio, A., Ketiemi, P., Nikulin, G., Panitz, H.J., Büchner, M., Stordal, F., Tazalika, L., 2013. Assessment of the performance of CORDEX regional climate models in simulating East African rainfall. *J. Clim.* 26, 8453–8475. doi:<https://doi.org/10.1175/JCLI-D-12-00708.1>.

Endris, H.S., Lennard, C., Hewitson, B., Dosio, A., Nikulin, G., Panitz, H.J., 2015. Teleconnection responses in multi-GCM driven CORDEX RCMs over Eastern Africa. *Clim. Dyn.* 46 (9–10), 2821–2846. doi:<https://doi.org/10.1007/s00382-015-2734-7>.

Favre, A., Stone, D., Cerezo, R., Philippon, N., Abiodun, B., 2011. Diagnostic of monthly rainfall from CORDEX simulations over Africa: focus on the annual cycles. In: Proc. Int. Conf. on the Coordinated Regional Climate Downscaling Experiment–CORDEX. World Climate Research Program, Trieste, Italy. <http://indico.ictp.it/event/a10131/session/63/contribution/52/material/0/0.pdf>, Accessed date: 2 April 2019.

Favre, A., Philippon, N., Pohl, B., Kalognomou, E., Lennard, C., Hewitson, B., Nikulin, G., Dosio, A., Panitz, H.J., Cerezo-Mota, R., 2015. Spatial distribution of precipitation annual cycles over South Africa in 10 CORDEX regional climate model present-day simulations. *Clim. Dyn.* 46 (3–6), 1799–1818. doi:<https://doi.org/10.1007/s00382-015-2677-z>.

Fotso-Nguemo, T.C., Vondou, D.A., Tchawoua, C., Haensler, A., 2017. Assessment of simulated rainfall and temperature from the regional climate model REMO and future changes over Central Africa. *Clim. Dyn.* 48 (11–12), 3685–3705. doi:<https://doi.org/10.1007/s00382-016-3294-1>.

Funk, C., Dettinger, M.D., Michaelsen, J.C., Verdin, J.P., Brown, M.E., Barlow, M., Hoell, A., 2008. Warming of the Indian Ocean threatens eastern and southern African food security but could be mitigated by agricultural development. *P. Natl. Acad. Sci. USA* 105, 11081–11086. doi:<https://doi.org/10.1073/pnas.0708196105>.

Gbobaniyi, E., Sarr, A., Sylla, M.B., Diallo, I., Lennard, C., Dosio, A., Dhiedi, Kamga, A.,

- Klutse, N.A.B., Hewitson, B., Nikulin, G., Lamptey, B., 2013. Climatology, annual cycle and interannual variability of precipitation and temperature in CORDEX simulations over West Africa. *Int. J. Climatol.* 34, 2241–2257. <https://doi.org/10.1002/joc.3834>.
- Giorgi, F., Gutowski, W.J., 2015. Regional dynamical downscaling and the CORDEX initiative. *Annu. Rev. Environ. Resour.* 40 (1), 467–490. <https://doi.org/10.1146/annurev-environ-102014-021217>.
- Giorgi, F., Jones, C., Asrar, G.R., 2009. Addressing climate information needs at the regional level: the CORDEX framework. *WMO Bull.* 58 (3), 175–183.
- Haensler, A., Saeed, F., Jacob, D., 2013. Assessing the robustness of projected precipitation changes over central Africa on the basis of a multitude of global and regional climate projections. *Clim. Chang.* 121 (2), 349–363. <https://doi.org/10.1007/s10584-013-0863-8>.
- Harris, I., Jones, P.D., Osborn, T.J., Lister, D.H., 2014. Updated high-resolution grids of monthly climatic observations – the CRU TS3.10 dataset. *Int. J. Climatol.* 34, 623–642. <https://doi.org/10.1002/joc.3711>.
- Hastenrath, S., Polzin, D., Mutai, C., 2011. Circulation mechanisms of Kenya rainfall anomalies. *J. Clim.* 24 (2), 404–412. <https://doi.org/10.1175/2010JCLI3599.1>.
- Hu, Q., Li, Z., Wang, L., Huang, Y., Wang, Y., Li, L., 2019. Rainfall Spatial Estimations: a review from spatial interpolation to multi-source data merging. *Water Resour. Res.* 11 (3), 579. <https://doi.org/10.3390/w11030579>.
- Indeje, M., Semazzi, F.H.M., 2000. Relationships between QBO in the lower equatorial stratospheric zonal winds and East African seasonal rainfall. *Meteorol. Atmos. Phys.* 73 (3–4), 227–244. <https://doi.org/10.1007/s007030050075>.
- Indeje, M., Semazzi, F.H.M., Ogallo, L.J., 2000. ENSO signals in East African rainfall seasons. *Int. J. Climatol.* 20 (1), 19–46. [https://doi.org/10.1002/\(SICI\)1097-0088\(200001\)20:1<19::AID-JOC449>3.0.CO;2-0](https://doi.org/10.1002/(SICI)1097-0088(200001)20:1<19::AID-JOC449>3.0.CO;2-0).
- IPCC, 2014. Climate change 2014: synthesis report. In: Pachauri, R.K., Meyer, L.A. (Eds.), Contribution of Working Groups I, II and III to the Fifth Assessment Report of the Intergovernmental Panel on Climate Change. IPCC, Geneva, Switzerland, pp. 151.
- Jacob, D., Petersen, J., Eggert, B., Alias, A., Christensen, O.-B., Bouvier, L.M., Braun, A., Colette, A., Déqué, M., Georgievski, G., Georgopoulou, E., Gobiet, A., Menut, L., Nikulin, G., Haensler, A., Hempelmann, N., Jones, C., Keuler, K., Kovats, S., Kröner, N., Kotlarski, S., Kriegsmann, A., Martin, E., van Meijgaard, E., Moseley, C., Pfeifer, S., Preuschmann, S., Radermacher, C., Radtke, K., Rechid, D., Rounsevell, M., Samuelsson, P., Somot, S., Soussana, J.-F., Teichmann, C., Valentini, R., Vautard, R., Weber, B., Yiou, P., 2014. EURO-CORDEX: new high resolution climate change projections for European impact research. *Reg. Environ. Chang.* 14 (2), 563–578. <https://doi.org/10.1007/s10113-013-0499-2>.
- Kalogonou, E.A., Lennard, C., Shongwe, M., Pinto, I., Favre, A., Kent, M., Hewitson, B., Dosio, A., Nikulin, G., Panitz, H.J., 2013. A diagnostic evaluation of precipitation in CORDEX models over southern Africa. *J. Clim.* 26 (23), 9477–9506. <https://doi.org/10.1175/JCLI-D-12-00703.1>.
- Kendall, M.G., 1975. *Rank Correlation Methods*, 4th ed. Griffin, London, pp. 202.
- Kent, C., Chadwick, R., Rowell, D.P., 2015. Understanding uncertainties in future-projections of seasonal tropical precipitation. *J. Clim.* 28, 4390–4413. <https://doi.org/10.1175/JCLI-D-14-00613.1>.
- Kisembo, J., Favre, A., Dosio, A., Lennard, L., Sabiti, G., Nimusiima, A., 2018. Evaluation of rainfall simulations over Uganda in CORDEX regional climate models. *Theor. Appl. Climatol.* 137 (1–2), 1117–1134. <https://doi.org/10.1007/s00704-018-2643-x>.
- Klutse, N.A.B., Sylla, M.B., Diallo, I., Sarr, A., Dosio, A., Diedhiou, A., Kamba, A., Lamptey, B., Ali, A., Gbobanyini, E., Owusu, K., Lennard, C., Hewitson, B., Nikulin, G., Panitz, H.J., Büchner, M., 2016. Daily characteristics of West African summer monsoon precipitation in CORDEX simulations. *Theor. Appl. Climatol.* 123 (1–2), 369–386. <https://doi.org/10.1007/s00704-014-1352-3>.
- Liebmann, B., Hoerling, M.P., Funk, C., Bladé, I., Dole, R.M., Allured, D., Quan, X., Pegion, P., Eischeid, J.K., 2014. Understanding recent Eastern Horn of Africa rainfall variability and change. *J. Clim.* 27, 8630–8645. <https://doi.org/10.1175/JCLI-D-13-00714.1>.
- Luhunga, P., Botai, J., Kahimba, F., 2016. Evaluation of the performance of CORDEX regional climate models in simulating present climate conditions of Tanzania. *J. Southern Hemisphere Earth Syst. Sci.* 66 (1), 32–54. <https://doi.org/10.22499/3.6601.005>.
- Maidment, R.I., Allan, R.P., Black, E., 2015. Recent observed and simulated changes in precipitation over Africa. *Geophys. Res. Lett.* 42, 8155–8164. <https://doi.org/10.1002/2015GL065765>.
- Manatsa, D., Morioka, Y., Behera, S.K., Matarira, C.H., Yamagata, T., 2014. Impact of mascarene high variability on the East African 'short rains'. *Clim. Dyn.* 42, 1259–1274. <https://doi.org/10.1007/s00382-013-1848-z>.
- Mann, H.B., 1945. Nonparametric tests against trend. *Econometrica* 13, 245–259.
- Maure, G., Pinto, I., Ndebele-Murisa, M., Muthige, M., Lennard, C., Nikulin, G., Meque, A., 2018. The southern African climate under 1.5 °C and 2 °C of global warming as simulated by CORDEX regional climate models. *Environ. Res. Lett.* 13 (6). <https://doi.org/10.1088/1748-9326/aab190>.
- Mukabana, J.R., Pielke, R.A., 1996. Investigating the influence of synoptic-scale monsoonal winds and mesoscale circulations on diurnal weather patterns over Kenya using a mesoscale numerical model. *Mon. Weather Rev.* 124, 224–243. [https://doi.org/10.1175/1520-0493\(1996\)124<0224:ITIOSS>2.0.CO;2](https://doi.org/10.1175/1520-0493(1996)124<0224:ITIOSS>2.0.CO;2).
- Mutayoba, E., Kashaigili, J.J., 2017. Evaluation for the performance of the CORDEX regional climate models in simulating rainfall characteristics over mbarali river catchment in the Ruffiji Basin, Tanzania. *J. Geosci. Environ. Protection* 5 (4), 139. <https://doi.org/10.4236/gep.2017.54011>.
- Nicholson, S.E., 2008. The intensity, location and structure of the tropical rainbelt over west Africa as factors in interannual variability. *Int. J. Climatol.* 28, 1775–1785. <https://doi.org/10.1002/joc.1507>.
- Nicholson, S.E., 2017. Climate and climatic variability of rainfall over eastern Africa. *Rev. Geophys.* 55 (3), 590–635. <https://doi.org/10.1002/2016RG000544>.
- Nicholson, S.E., Kim, J., 1997. The relationship of the El Niño–Southern oscillation to African rainfall. *Int. J. Climatol.* 17 (2), 117–135. [https://doi.org/10.1002/\(SICI\)10970088\(199702\)17:2<117::AID-JOC84>3.0.CO;2-O](https://doi.org/10.1002/(SICI)10970088(199702)17:2<117::AID-JOC84>3.0.CO;2-O).
- Nicholson, S.E., Selato, 2000. The influence of La Niña on Africa rainfall. *Int. J. Climatol.* 20, 1761–1776. [https://doi.org/10.1002/1097-0088\(20001130\)20:14<1761::AID-JOC580>3.0.CO;2-W](https://doi.org/10.1002/1097-0088(20001130)20:14<1761::AID-JOC580>3.0.CO;2-W).
- Nikulin, G., Jones, C., Giorgi, F., Asrar, G., Büchner, M., Cerezo-Mota, R., Christensen, O.B., Déqué, M., Fernandez, J., Hänsler, A., van Meijgaard, E., 2012. Precipitation climatology in an ensemble of CORDEX-Africa regional climate simulations. *J. Clim.* 25 (18), 6057–6078. <https://doi.org/10.1175/JCLI-D-11-00375.1>.
- Oettli, P., Camberlin, P., 2005. Influence of topography on monthly rainfall distribution over East Africa. *Clim. Res.* 28 (3), 199–212. <https://doi.org/10.3354/cr028199>.
- Ogwang, B.A., Chen, H., Li, X., Gao, C., 2014. The Influence of topography on East African October to December climate: sensitivity experiments with RegCM4. *Adv. Meteorol.* 2014, ID 143917. doi:<https://doi.org/10.1155/2014/143917>.
- Ogwang, B.A., Ongoma, V., Li, X., Ogou, F.K., 2015. Influence of mascarene high and Indian Ocean dipole on East African extreme weather events. *Geogr. Pannonica* 19, 64–72.
- Ongoma, V., Chen, H., 2017. Temporal and spatial variability of temperature and precipitation over East Africa from 1951 to 2010. *Meteorol. Atmos. Phys.* 129 (2), 131–144. <https://doi.org/10.1007/s00703-016-0462-0>.
- Ongoma, V., Chen, H., Gao, C., 2018. Projected change in mean rainfall and temperature over East Africa based on CMIP5 Models. *Int. J. Climatol.* 38, 1375–1392. <https://doi.org/10.1002/joc.5252>.
- Ongoma, V., Chen, H., Gao, C., 2019. Evaluation of CMIP5 twentieth century rainfall simulation over the equatorial East Africa. *Theor. Appl. Climatol.* 135 (3–4), 893–910. <https://doi.org/10.1007/s00704-018-2392-x>.
- Osima, S., Indasi, V.S., Zaroug, M., Endris, H.S., Gudoshava, M., Misiani, H.O., Nimusiima, A., Anyah, R.O., Otieno, G., Ogwang, B.A., Jain, S., Kondowe, A.L., Mwangi, E., Lennard, C., Nikulin, G., Dosio, A., 2018. Projected climate over greater horn of Africa under 1.5°C and 2°C global warming. *Environ. Res. Lett.* 13 (6). <https://doi.org/10.1088/1748-9326/aaba1b>.
- Owiti, Z., Ogallo, L.A., Mutemi, J., 2008. Linkages between the Indian Ocean dipole and east African seasonal rainfall anomalies. *J. Kenya Meteorol. Soc.* 2, 3–17.
- Pal, J.S., Giorgi, F., Bi, X., Elguindi, N., Solmon, F., Gao, X., Rauscher, S.A., Francisco, R., Zakey, A., Winter, J., Ashfaq, M., Syed, F.S., Bell, J.L., Diffenbaugh, N.S., Karmacharya, J., Konaré, A., Martinec, D., da Rocha, R.P., Sloan, L.C., Steiner, A.L., 2007. Regional climate modeling for the developing world: the ICTP RegCM3 and RegCM2. *Bull. Am. Meteorol. Soc.* 88, 1395–1409. <https://doi.org/10.1175/BAMS-88-9-1395>.
- Pinto, I., Lennard, C., Tadross, M., Hewitson, B., Dosio, A., Nikulin, G., Panitz, H.-J., Shongwe, M.E., 2015. Evaluation and projections of extreme precipitation over southern Africa from two CORDEX models. *Clim. Chang.* 135 (3–4), 655–668. <https://doi.org/10.1007/s10584-015-1573-1>.
- Pohl, B., Camberlin, P., 2006. Influence of the Madden–Julian oscillation on East African rainfall. I: intraseasonal variability and regional dependency. *Q. J. R. Meteorol. Soc.* 132, 2521–2539. <https://doi.org/10.1256/qj.05.104>.
- Russo, S., Sillmann, J., Fischer, E.M., 2015. Top ten European heatwaves since 1950 and their occurrence in the coming decades. *Environ. Res. Lett.* 10 (12), 124003. <https://doi.org/10.1088/1748-9326/10/12/124003>.
- Saji, N.H., Goswami, B.N., Vinayachandran, P.N., Yamagata, T., 1999. A dipole mode in the tropical Indian Ocean. *Nature* 401, 360–363. <https://doi.org/10.1038/43854>.
- Samuelsson, P., Jones, C.G., Willén, U., Ullerstig, A., Gollvik, S., Hansson, U., Hansson, U., Jansson, C., Kjellström, E., Nikulin, G., Wyser, K., 2012. The rossby centre regional climate model RCA3: model description and performance. *Tellus A* 63, 4–23. <https://doi.org/10.1111/j.1600-0870.2010.00478.x>.
- Segele, Z.T., Leslie, L.M., Lamb, P.J., 2009. Evaluation and adaptation of a regional climate model for the horn of Africa: rainfall climatology and interannual variability. *Int. J. Climatol.* 29 (1), 47–65. <https://doi.org/10.1002/joc.1681>.
- Shongwe, M.E., van Oldenborgh, G.J., van den Hurk, B., van Aalst, M., 2011. Projected changes in mean and extreme precipitation in Africa under global warming. part II: East Africa. *J. Clim.* 24, 3718–3733. <https://doi.org/10.1175/2010JCLI2883.1>.
- Souvereinjs, N., Thiery, W., Demuzere, M., Van Lipzig, N.P.M., 2016. Drivers of future changes in East African precipitation drivers of future changes in East African precipitation. *Environ. Res. Lett.* 11 (11), 114011. <https://doi.org/10.1088/1748-9326/11/11/114011>.
- Stensrud, D.J., 2007. *Parametrization Schemes: Keys to Understanding Numerical Weather Prediction Models*. Cambridge University Press, Cambridge, UK, pp. 480.
- Strandberg, G., Bärring, L., Hansson, U., Jansson, C., Jones, C., Kjellström, E., Kupiainen, M., Nikulin, G., Samuelsson, P., Ullerstig, A., 2014. CORDEX scenarios for Europe from the rossby centre regional climate model RCA4. In: Technical Report. vol. 116 Climate Research Rossby Centre.
- Sylla, M.B., Diallo, I., Pal, J.S., 2013. West African monsoon in state-of-the-art regional climate models. In: Tarhule, A. (Ed.), *Climate Variability-Regional and Thematic Patterns*. 980-953-307-816-3.
- Tamoffo, A.T., Moufouma-Okia, W., Dosio, A., James, R., Pokam, W.M., Vondou, D.A., Nouayou, R., 2019. Process-oriented assessment of RCA4 regional climate model projections over the Congo Basin under 1.5°C and 2°C global warming levels: influence of regional moisture fluxes. *Clim. Dyn.* <https://doi.org/10.1007/s00382-019-04751-y>.
- Taylor, K.E., Stouffer, R.J., Meehl, G.A., 2012. An overview of CMIP5 and the experiment design. *Bull. Am. Meteorol. Soc.* 93, 485–498. <https://doi.org/10.1175/BAMS-D-11-00094.1>.
- Tramblay, Y., Ruelland, D., Somot, S., Bouaicha, R., Servat, E., 2013. High-resolution Med-CORDEX regional climate model simulations for hydrological impact studies: a

- first evaluation of the ALADIN-Climate model in Morocco. *Hydrol. Earth Syst. Sci.* 17, 3721–3739. <https://doi.org/10.5194/hess-17-3721-2013>.
- Unden, P., Rontu, L., Jinen, H., Lynch, P., Calvo, J., Cats, G., Cuxart, J., Eerola, K., Fortelius, C., Garcia-Moya, J.A., Jones, C., Geert Lenderlink, G., McDonald, A., Mcgrath, R., Navascues, B., Nielsen, N.W., Degaard, V., Rodriguez, E., Rummukainen, M., Sattler, K., Sass, B.H., Savijarvi, H., Schreur, B.W., Sigg, R., 2002. HIRLAM-5 Scientific Documentation. https://repositorio.aemet.es/bitstream/20.500.11765/6323/1/HIRLAMSciDoc_Dec2002.pdf, Accessed date: 25 March 2019.
- Vondou, D.A., Haensler, A., 2017. Evaluation of simulations with the regional climate model REMO over Central Africa and the effect of increased spatial resolution. *Int. J. Climatol.* 37, 741–760. <https://doi.org/10.1002/joc.5035>.
- Warnatzsch, E.A., Reay, D.S., 2019. Temperature and precipitation change in Malawi: evaluation of CORDEX-Africa climate simulations for climate change impact assessments and adaptation planning. *Sci. Total Environ.* 654, 378–392. <https://doi.org/10.1016/j.scitotenv.2018.11.098>.
- Wilby, R.L., Fowler, H.J., 2010. Regional climate downscaling. In: Fung, C.F., Lopez, A., New, M. (Eds.), *Modelling the Impact of Climate Change on Water Resources*. Wiley-Blackwell Publishing, Chichester.
- Wilks, S.D., 2006. *Statistical methods in the Atmospheric Science*, 2nd edn. Academic Press.
- Williams, A.P., Funk, C., Michaelsen, J., Rauscher, S.A., Robertson, I., Wils, T.H.G., Koprowski, M., Eshetu, Z., Loader, N.J., 2012. Recent summer precipitation trends in the greater horn of Africa and the emerging role of Indian Ocean sea surface temperature. *Clim. Dyn.* 39, 2307–2328. <https://doi.org/10.1007/s00382-011-1222-y>.
- World Bank, 2012. *Doing business in the East African economies*. IFC/World Bank Rep. 116.